

The Evolution of the Water Distribution in a Viscous Protoplanetary Disk

Fred J. Ciesla* and Jeffrey N. Cuzzi

*Author to whom correspondence should be addressed

NASA Ames Research Center; MS 245-3; Moffett Field, CA 94043
ciesla@cosmic.arc.nasa.gov, voice:(650) 604-0328, fax:(650) 604-6779

pages: 44
tables: 3
figures: 7

Abstract

Astronomical observations have shown that protoplanetary disks are dynamic objects through which mass is transported and accreted by the central star. This transport causes the disks to decrease in mass and cool over time, and such evolution is expected to have occurred in our own solar nebula. Age dating of meteorite constituents shows that their creation, evolution, and accumulation occupied several Myr, and over this time disk properties would evolve significantly. Moreover, on this timescale, solid particles decouple from the gas in the disk and their evolution follows a different path. It is in this context that we must understand how our own solar nebula evolved and what effects this evolution had on the primitive materials contained within it. Here we present a model which tracks how the distribution of water changes in an evolving disk as the water-bearing species experience condensation, accretion, transport, collisional destruction, and vaporization. Because solids are transported in a disk at different rates depending on their sizes, the motions will lead to water being concentrated in some regions of a disk and depleted in others. These enhancements and depletions are consistent with the conditions needed to explain some aspects of the chemistry of chondritic meteorites and formation of giant planets. The levels of concentration and depletion, as well as their locations, depend strongly on the combined effects of the gaseous disk evolution, the formation of rapidly migrating rubble, and the growth of immobile planetesimals. Understanding how these processes operate simultaneously is critical to developing our models for meteorite parent body formation in the solar system and giant planet formation throughout the galaxy. We present examples of evolution under a range of plausible assumptions and demonstrate how the chemical evolution of the inner region of a protoplanetary disk is intimately connected to the physical processes which occur in the outer regions.

Keywords: Origin, Solar System; Solar Nebula; Meteorites; Cosmochemistry; Planetary Formation

1 Introduction

The solar system contains a wide variety of objects, ranging from small, rocky bodies at relatively small heliocentric distances to huge, gaseous planets at tens of astronomical units from the sun. The characteristics of these objects were determined billions of years ago, when they accreted from primitive material that was present in their respective formation regions. The properties of these primitive materials were set by the physical and chemical environments that they were exposed to prior to accretion. A long standing goal in studying primitive objects has been to identify what these environments were and how they varied with location and time in the solar nebula.

Observations of protoplanetary disks around young stars have shown that unraveling the chemical and physical structure of such disks requires understanding how they evolve over time. Measurements of the excess radiation being emitted from young stars show that they are accreting mass at rates up to $10^{-6} M_{\odot}/\text{yr}$, decreasing with time (Calvet *et al.*, 2005). This mass is being fed onto the stars through the disks that surround them, implying that these disks are dynamic objects. While the driving mechanism for this mass transport has not been identified, we realize that the disks grow less massive and cooler over time. It is in this dynamic, evolving setting that we must understand what physical and chemical environments existed in the solar nebula and how they affected the primitive materials within them.

In order to understand the various conditions that exist within a protoplanetary disk, it is necessary to identify the timescales over which the environments within it change and the timescales over which material is transported from one region to another. In this paper, we illustrate how this mixing and transport take place by investigating how the distribution of water changes within an evolving disk due to the different processes identified above. We focus on water due to its importance in many different aspects of the formation of our solar system. In the outer solar nebula, water is expected to have been a major condensable, making up approximately 50% of the mass of solids. In the hot, inner solar nebula, water would be found in the vapor phase and its concentration determined the oxidation state of the gas and controlled the chemistry that took place and the mineralogy of even high-temperature solids. The boundary between these two regions is called the “snow line,” and refers to the location outside of which water freezes out to form a solid. Where this transition took place, and how water was incorporated into solids, are also important to understand so that we can identify how Earth and other habitable planets acquired their water contents.

The new model of the distribution of water in a protoplanetary disk outlined here considers the formation, growth, and destruction of solid water particles and vapor by collisions, vaporization, and condensation while simultaneously tracking their transport in an evolving disk. Our model also self-consistently tracks the change in opacity of the disk due to the transport of the solids within it, an effect that is often neglected in disk evolution models. In developing this model, we build upon a suite of previous studies that are reviewed in Section 2. The models for global nebular evolution and the water distribution are outlined in Sections 3 and 4 respectively. Results of some model runs are presented in Section 5. The implications of these results for the chemical evolution of primitive solids, the formation of giant planets, and protoplanetary disk studies are discussed in Section 6. In section 7, we outline our conclusions and discuss future work needed to better improve our understanding of water transport in the solar nebula.

2 Previous Models of Water Transport in the Solar Nebula

Solids and vapor within a protoplanetary disk can be transported in a number of ways. Diffusion of material along concentration gradients is expected to occur regardless of the mechanism responsible for driving disk evolution (Morfill and Völk, 1984; Stevenson and Lunine, 1988; Hersant *et al.*, 2001; Gail, 2001; Takeuchi and Lin, 2002; Cuzzi *et al.*, 2003; Cuzzi and Zahnle, 2004; Boss, 2004; Keller and Gail, 2004). In addition, the structure of the disk itself will lead to the transport of materials. The gas in the disk will generally be supported in the radial direction by a pressure gradient, reducing the effective gravity that the gas feels in its orbit around the sun and causing it to move at slightly less than Keplerian speed. Solids do not feel this gradient and attempt to follow Keplerian orbits, resulting in the solids experiencing a headwind due to the velocity difference between them and the gas. The solids thus lose energy and angular momentum to the gas, and move inwards over time. The velocities with which these transport processes operate are described below (for more details, see Cuzzi and Weidenschilling, 2005). Here we review previous work that has studied the effects of these transport processes on how water would be distributed in the solar nebula.

Stevenson and Lunine (1988) investigated the diffusion of water vapor from the inner solar nebula to the snow line as a way of locally increasing the density of solids in order to facilitate the rapid growth of Jupiter's core. Upon reaching the snow line, water vapor was assumed to condense into ice and be accreted by pre-existing planetesimals located there. It was found that the diffusional redistribution of the water vapor resulted in an increase in the surface density of solids immediately outside the snow line by a factor of ~ 75 in roughly 10^5 years. This enhancement of solids would then allow Jupiter's massive core to grow much more rapidly than if the core had to grow from the canonical amount of solids locally present. Morfill and Völk (1984) on the other hand, did not assume material was trapped on immobile planetesimals, so their solutions did not show these substantial effects.

Cyr *et al.* (1998) extended this model to examine the diffusion of water vapor along with the migration of the freshly formed ice particles into the inner nebula *via* gas drag. As the ice particles drifted inwards, they vaporized at a finite rate (Lichtenegger and Komle, 1991) and could drift significant distances inwards before completely vaporizing. This drift of the particles served as a way of replenishing water vapor to the inner nebula, though Cyr *et al.* (1998) found that the eventual accumulation of the condensed particles onto planetesimals would halt this inward migration and still lead to the complete dehydration of the inner solar nebula in $\sim 10^5$ years. After this time, the concentration of solids beyond the snow line would increase to roughly the same amount as found by Stevenson and Lunine (1988).

Both Stevenson and Lunine (1988) and Cyr *et al.* (1998) focused on the region of the nebula inside the snow line, ignoring the effects of particles migrating from the outer nebula inwards, as well as the evolving nature of the solar nebula. Stepinski and Valageas (1997) considered the distribution of water throughout an extended evolving nebula (~ 200 AU). In this model, the authors calculated the growth of particles as they collided with one another, and their subsequent movement due to diffusion and gas drag. They also calculated the simultaneous evolution of the viscous protoplanetary disk, accounting for the changes in surface density and temperature. They reached similar conclusions to Stevenson and Lunine (1988) and Cyr *et al.* (1998) in that a large pile-up of ice would occur just outside of the snow line. If massive, compact (extending to ~ 20 AU) disks were investigated, the solids rapidly migrated to the inner region of the disk before

planetesimals could form and were lost. The extended (~ 200 AU) disk ensured that solids would have to migrate over large distances and were more likely get incorporated into large, immobile planetesimals before being lost.

Due to the complexity of the different processes involved, Stepinski and Valageas (1997) made a number of simplifying assumptions in developing their model. In this treatment, the authors allowed for only one size of particles to exist at a given distance from the sun. Models for the growth of bodies in the solar nebula (e.g. Weidenschilling, 1980, 1984, 1997, 2000; Weidenschilling and Cuzzi, 1993; Dullemond and Dominik, 2005) have shown that a range of particle sizes would exist at a given location in the nebula. As will be discussed below, different sized objects will have very different dynamical behaviors in a viscous disk that must be taken into account. Also, Stepinski and Valageas (1997) assumed that all collisions between solids led to accretion (perfect sticking), and they found that more turbulent disks lead to more rapid growth of particles. This treatment contradicts detailed work done by other authors which suggests that turbulence hinders growth and that even moderate turbulence may cause meter-sized bodies to destroy one another in collisions (e.g. Cuzzi and Weidenschilling, 2005). Finally, to determine the temperatures of the nebula at every location, Stepinski and Valageas (1997) determined the opacity for the disk assuming a solar abundance of elements at a given location. As will be shown below, the rapid transport of material within a disk will result in all locations in the nebula departing from a solar composition. This would lead to variations in the opacity in the disk, which in turn, will affect its physical evolution.

Cuzzi and Zahnle (2004) developed a model to track the evolution of a “vaporizing” species in a protoplanetary disk (taken here to be water). They provided an analytic solution to an equation describing the simultaneous diffusion of vapor and dust along with the inward migration of meter-sized bodies throughout the nebula for steady-state cases. These authors found that before the inner nebula would be dehydrated as other studies had found, it could possibly go through a period where it was enhanced in water vapor. This concept was first explored in the context of silicates by Cuzzi *et al.* (2003). Cuzzi and Zahnle (2004) argued that until planetesimals grow outside the snow line, bodies from the outer nebula will continuously migrate into the inner nebula and vaporize, enriching the gas with water and suggest that this could explain the presence of oxidized species in primitive meteorites. Once the immobile planetesimals form, they act as a sink by accreting material rather than allowing it to drift inwards, and the inner nebula begins to dehydrate as was found by Stevenson and Lunine (1988) and Cyr *et al.* (1998).

In doing their calculations, Cuzzi and Zahnle (2004) also made a number of simplifying assumptions. The goal was to illustrate the different phases of evolution that the solar nebula may have experienced due to volatile transport, not to explicitly model it. Thus they only considered a snapshot of the nebula when the snow line existed at a fixed location, assumed that the meter-sized bodies represented a fixed fraction of the total solids, and did not consider accretion or destruction of those bodies. In a real protoplanetary disk, these disk and particle characteristics will change over time, often on very different timescales, and will affect how the water distribution evolves. In addition, Cuzzi and Zahnle (2004) assumed that there was an infinite reservoir of solids in the outer nebula, providing enough material for the inner nebula to become significantly enhanced (up to several orders of magnitude, depending on parameters), though the authors state that this assumption requires detailed numerical testing.

The work reviewed thus far has provided insight into the different processes that would affect the distribution of water vapor in the solar nebula and has offered explanations of how Jupiter’s

core formed so quickly and of the origin of the different oxidation states recorded by the various meteorite classes. The goal here is to develop an internally consistent model which incorporates the concepts explored in these earlier papers and is more consistent with detailed studies of particle growth in protoplanetary disks.

In developing the model presented here, we, too, had to make some simplifying assumptions as will be discussed below. The variables needed to describe the model are listed in Table 1. Despite the attempts to make this model completely self-consistent and dependent only on well understood physics, a set of parameters must be introduced, which, unfortunately, are relatively unconstrained by observations (Table 2). They represent estimates as to what the structure of a protoplanetary disk may be and the evolutionary processes that occur within it. They are assumed to be constant in both space and time (unless otherwise stated), though there is no reason to believe that is the case. Due to these uncertainties, the results presented here do not represent specific, quantitative predictions of the behavior of water in a protoplanetary disk. Instead, they should be interpreted as global trends for disks in general which provide us with a context within which we can understand how materials are distributed in protoplanetary disks and, hopefully, help interpret some observations. Specific applications will be discussed in detail at the end of this paper.

3 Evolution of the Nebular Gas

As described above, astronomical observations suggest that protoplanetary disks are evolving objects, with mass being transported within them (Calvet *et al.*, 2000, 2005). The exact driving mechanism for this evolution is unknown and is the subject of ongoing research. Proposed mechanisms include turbulence induced viscosity (Shakura and Sunyaev, 1973; Pringle, 1981; Lin and Papaloizou, 1985; Ruden and Pollack, 1991; Stepinski, 1998) where the turbulence arises from either magnetohydrodynamical or shear instabilities (Balbus and Hawley, 1991; Gammie, 1996; Huré *et al.*, 2001; Davis, 2003; Richard and Davis, 2004) or wave-driven gravitational torques (Laughlin and Rozyczka, 1996; Boss, 2004). It is possible that more than one mechanism played a role at various times and locations over the lifetime of a disk.

Here we use the α -viscosity model to describe the evolution of the disk over the course of millions of years. This is done without prejudice as to the source of α and in lieu of the β -viscosity model (Richard and Zahn, 1999; Richard and Davis, 2004) for simplicity and in order to facilitate comparisons to other work. This model assumes that the evolution of the disk is caused by a viscosity that arises as a result of turbulent motions within the gas. In this prescription, the surface density of the gas is governed by the equation:

$$\frac{\partial \Sigma}{\partial t} = \frac{3}{r} \frac{\partial}{\partial r} \left[r^{\frac{1}{2}} \frac{\partial}{\partial r} \left(\Sigma \nu r^{\frac{1}{2}} \right) \right] \quad (1)$$

where Σ is the total surface density of the disk, ν is the kinematic viscosity, and r is the radius from the central star (the star is assumed to grow negligibly in mass over the lifetime of the disk).

In the α -disk model, the kinematic viscosity is assumed to be a function of nebular parameters and can be described by the equation:

$$\nu = \alpha c_s H \quad (2)$$

where c_s is the local speed of sound and H is the local nebular scale height. The turbulence parameter α is assumed to be some value, generally much less than 1 (Lin and Papaloizou, 1985; Ruden and Pollack, 1991). For simplicity, and due to the few constraints placed on it, α is generally assumed to be both temporally and spatially constant.

The local speed of sound is given by:

$$c_s = \left(\frac{\gamma k T_m}{\bar{m}} \right)^{\frac{1}{2}} \quad (3)$$

where γ is the ratio of specific heats for the gas (taken to be 1.4 here), k is Boltzmann's constant, T_m is the temperature of the nebula at the midplane, and \bar{m} is the average molecular weight of the gas (taken to be 4×10^{-24} g to account for the gas being composed of mainly H_2 and He). The disk scale height is related to the speed of sound by:

$$H = \frac{c_s}{\Omega} \quad (4)$$

where Ω is the angular rotation frequency of a Keplerian orbit at the radial distance of interest.

The thermal structure of the nebula is determined by balancing the combination of the local viscous dissipation and stellar irradiation with the radiative energy loss from the surfaces of the disk. That is:

$$2\sigma \left(T_e^4 - T_{irr}^4 - T_{amb}^4 \right) = \frac{9}{4} \Sigma \nu \Omega^2 \quad (5)$$

where σ is the Stefan-Boltzmann constant and T_e is the effective temperature of the surface of the disk. Here, T_{irr} is the temperature at the surface of the disk determined by irradiation from the central star and T_{amb} is the ambient temperature from the local environment in which the disk is located. The irradiation temperature is determined by assuming that the disk is flat:

$$T_{irr}^4(r) = \frac{2}{3\pi} T_*^4 \left(\frac{R_*}{r} \right)^3 \quad (6)$$

where T_* and R_* are the surface temperature and radius of the central object, taken to be 4000 K and $3R_\odot$ respectively (Ruden and Pollack, 1991). The ambient temperature, T_{amb} is assumed to be some low constant value, set to 20 K in the work presented here to represent minimal effects from outside sources. By using a low value for the assumed ambient temperature we are concentrating on how the disk evolves due to the effects of internal processes. It has recently been suggested that the sun may have formed in close proximity to a massive star, which would have led to a hotter ambient radiation field (and thus higher midplane temperatures) as well as other external perturbations (Hester and Desch, 2005). Such effects should be considered in future work.

The effective temperature can be related to the midplane temperature by the equation:

$$T_m^4 = \frac{3}{4} \tau T_e^4 \quad (7)$$

where τ is the optical depth from the midplane of the nebula to the surface. This is given by:

$$\tau = \frac{\kappa \Sigma}{2} \quad (8)$$

where κ is the local opacity of the disk.

For these initial models we wanted to adopt an opacity prescription which was simple, and avoided the huge uncertainties currently facing most treatments. The opacity in question is a Rosseland mean opacity; that is, wavelength averaged and weighted by local thermal radiation. Many models simply adopt the Rosseland mean opacities of Pollack *et al.* (1994), which display explicit temperature dependence for two reasons. First, absorption edges appear at temperatures where different major species (water, organics, silicates) evaporate and the opacity thereby drops; second, a different kind of temperature dependence appears at low temperatures because of the decreasing absorption efficiency of the grains they modeled as the effective wavelength gets much larger than the grain size. Pollack *et al.* (1994) assumed a composition of roughly 1/3 water, 1/3 moderately refractory organics, and 1/3 silicates; this leads to a negligible opacity drop where water evaporates but large ones where the postulated organics and silicates evaporate. The most frequently used results of Pollack *et al.* assume a MRN size distribution (Mathis *et al.*, 1977), which is a steep powerlaw extending only to 5 micron radius, but in which practically all the scattering mass and area is in the smallest particles - hence the low-temperature, long-wavelength temperature dependence. Cassen (1994) simplified the results of Pollack *et al.*, retaining only the silicate evaporation opacity drop (and the low-temperature dependence) - thus still assuming tiny grains ($\ll 30$ micron radius), which sets the magnitude of the opacity.

Clearly, since $\kappa \sim \pi a^2/m \sim 1/a\rho$, opacities drop as grains grow. Miyake and Nakagawa (1993) illustrate how particle growth affects grain opacity. Once particles become opaque to thermal radiation (in their cases, around 10 micron radius), opacity drops by an order of magnitude for each order of magnitude change in radius. Moreover, all grain accretion models indicate that grain growth from ISM grain size to *at least* 100 micron radius is quite easy and quite rapid in the nebula, because of the low relative velocities and high densities (Weidenschilling 1997, Cuzzi and Weidenschilling 2005). Thus one can surely overestimate opacities significantly by adopting opacities that simply assume micron-sized grains. On the other hand, these initial aggregates are also probably quite 'fluffy' so their individual *mass* is much smaller than one might expect for a solid particle of the same size; that is, if they grow as fractals (Meakin and Donn, 1988; Beckwith *et al.*, 2000), the product $a\rho$ is the same as that for an independent, micron-size monomer constituent and their opacity is the same. Compaction, of course, will change this, so growth to larger sizes has a very large potential effect. Particle radii of several cm, still included in our "dust" population, are quite probably compacted and have opacities orders of magnitude smaller than those frequently used (Pollack *et al.* 1994, Cassen 1994). Complicating things still further is the as-yet unmodeled evolving size distribution itself over these long times and large radial ranges - including particle growth, collisions, erosion, and destruction, which are here simply modeled by our three crude size bins and the total amount of mass in the "dust" population itself (the opacity of the migrators and the planetesimals is negligible). Point models such as Weidenschilling (1997) would be prohibitive to run in a model such as ours. Yet, this evolution surely does occur. Miyake and Nakagawa (1993, figure 10) show that the opacities for size distributions of realistic, porous particles ranging in size from 0.01μ to 10cm radius vary by three orders of magnitude, even depending on the slope of their powerlaw size distribution (different slopes emphasize either the smaller or the larger particles). The several cm^2g^{-1} (per gram of nebula gas, that is) of Pollack *et al.* (1994) and Cassen (1994) are at the high end of this range.

Where, then, does this leave us regarding an opacity model for our evolving disk? Fortunately, the midplane temperature depends only weakly on the total optical depth ($T_m \propto \tau^{1/4}$); factors

of several will only change the timing and location of the water evaporation front we want to model, not change the fact that there *is* a water evaporation front. Our focus is not on its specific location, but the phenomena associated with its presence. The likelihood of significant particle growth leads us to doubt the reality of the T^2 dependence found by Pollack et al (1994) and assumed by Cassen (1994), which is a tiny-particle property, so we will assume a temperature-independent opacity per gram of *solid material*. Results of Weidenschilling (1997, 2000) using detailed particle growth models, tend to find the “dust” regime (microns to tens of centimeters radius) has a mass distribution $m(a)$ with equal mass per bin of width a (equal to the particle radius); that is, then, $n(a) a^4 = \text{constant}$, or $n(a) \propto a^{-4}$. From figure 10 of Miyake and Nakagawa (1993) we see that, *very* roughly, the opacity of such a distribution, ranging from microns to centimeters, can be approximated by something like Cassen’s adopted $5 \text{ cm}^2\text{g}^{-1}$ (because the steep powerlaw emphasizes particles at the small end of the range), over the wavelength range $1\text{-}100\mu\text{m}$ characterizing nebula blackbody radiation. This opacity assumes a full nebula relative abundance of solids (ice plus silicate $\sim 1\%$ by mass assumed by Miyake and Nakagawa). We will adopt this value, with the advantage of making comparisons with prior work easier. It does indeed seem to be consistent with a realistic case. Thus, our local opacity is given by

$$\kappa = 5 \left[\frac{\Sigma_d(\text{H}_2\text{O})}{0.0045\Sigma} \right] \text{ cm}^2\text{g}^{-1} \quad (9)$$

where the opacity is given per gram of nebula gas having local surface mass density Σ . Because we are only tracking the ice component of material in the outer disk, the opacity relation is scaled by the ice mass fraction (0.0045, Krot *et al.*, 2000), and the assumption is made that the other solids closely follow the ice distribution. The dust population can be enhanced or depleted relative to “cosmic abundance.” As noted earlier, the opacity of the migrator and planetesimal populations is negligible. Inside of the water evaporation front, only silicate (and refractory organic) dust remains, which we do not specifically track in our model. Thus between the ice and silicate evaporation fronts we assume cosmic abundance of refractory materials, all in the “dust” size bin, with an average mass density (silicate + refractory organics/2) of $\sim 0.005\Sigma$, giving an opacity of $2.5 \text{ cm}^2\text{g}^{-1}$. More complicated models can be imagined, in which the very process which brings migrators inside the water evaporation front to evaporate also releases additional refractory dust (Cuzzi *et al.*, 2005), but we will not model that in this paper. To help with numerical stability while keeping the models plausible, a small opacity ($0.1 \text{ cm}^2\text{g}^{-1}$) is retained inside of the silicate evaporation front (1350-1400K). Physically, this is associated with (a) the refractory Calcium-Aluminum-rich material, about 5% of all silicates by mass, which survives to approximately 2000K (inside of which our model is insensitive to the opacity), and (b) some small amount of normal silicate material which will remain solid at high elevations, where the temperature decreases below the silicate condensation temperature.

One final refinement is added, because it deals expressly with the water evaporation front. The strong enhancement of water vapor just inside the water evaporation front, due to migrators evaporating near the *midplane*, will lead to condensation of additional “snow” at high elevations there where temperatures decrease below the water condensation temperature (Cassen, 1994; Davis, 2005). Because of the large amounts of water involved, this effect can result in noticeable opacity increases and outward displacement of the water evaporation front relative to a case where it is neglected. To model this effect we determine what surface density of ice-rich gas is needed in order to produce a midplane temperature of 160 K. The opacity of that gas is assumed to be given

by the above relation, with the water in the vapor phase also contributing to the opacity (at the higher elevations this vapor will indeed condense out to form “snow”). We determine the amount of gas needed by setting $T_m=160$ K, and using equations 5-8 to solve for the needed surface density. This represents the column density of material at the very upper layers of the disk which would contain condensed ice. The opacity of the rest of the gas in the column would be provided only by the silicates in this region, as temperatures would be high enough for water to exist only as a vapor which does not contribute significantly to the opacity. The opacity for the column is then found by a weighted average:

$$\kappa_{mean} = \left(2.5\Sigma_{T>160} + 5 \frac{(\Sigma_{vap} + \Sigma_d)}{0.0045\Sigma} \Sigma_{T<160} \right) \frac{1}{\Sigma} \quad (10)$$

where $\Sigma_{T<160}$ is the surface density of material at temperatures below 160 K, and $\Sigma_{T>160}$ is the remaining surface density at a given location of the disk.

4 Evolution of the Water Distribution

In this model, water exists in two phases: as vapor and as solids. The solid material considered here is divided into three categories: dust, migrators, planetesimals. Each of these categories represents a range of sizes of the solids, characterized by some *typical size*, and the evolution of these categories is calculated by assuming all the mass in each category is contained in particles of that single size. Here we aim to show the general evolution of how water vapor and ice could be distributed in protoplanetary disks by modeling all of the physics that control the evolution of the four species which have the most distinct dynamical behavior. Thus our model is an improvement over the single-size model at a given location of Stepinski and Valageas (1997), but is simpler to evolve than the full size distribution of Weidenschilling (1997) (or other similar studies) and accounts for the diversity of physical behaviors involved.

In general, water vapor will be transported by the same processes that transport the rest of the nebular gas (diffusion and advection). The transport of solids, on the other hand, will depend on the size of the solids under consideration. The dynamical evolution of a solid is determined by its Stokes number, St , which is the ratio of the particle stopping time to the turnover time of the largest local turbulent eddy (usually taken to be the local orbital period). The stopping time, t_s , measures the amount of time it takes for a particle to lose its relative velocity with respect to the gas and is given by $a\rho/\rho_g c_s$ for small particles ($a \ll \lambda$) and $a^2\rho/\rho_g c_s \lambda$ for larger objects, where a is the radius, λ is the mean free path in the gas, and ρ is the density of the particle. Dust particles represent those solids with $St \ll 1$, which covers solids with $a < 1$ cm. Because of their short stopping times, these particles are very well coupled to the gas. Planetesimals are those solids with $St \gg 1$, corresponding to bodies larger than 1 km. Due to their large inertia, planetesimal motions are relatively unaffected by the presence of the gas. Migrators are those particles in between with $St \sim 1$, corresponding to objects roughly 1 meter in size (Cuzzi and Weidenschilling, 2005). These bodies are most dramatically affected by gas drag as will be discussed below.

Here we present the equations which describe how water vapor, dust, migrators, and planetesimals behave in a viscous accretion disk. We first present the equations which describe the transport of the various species, with each equation including a term representing the net sources

and sinks for the respective species. The sources and sinks represent the transfer of mass from one species to another through accretion, collisional destruction, vaporization, or condensation, as described below.

4.1 Water Vapor

The major transport mechanisms of water vapor will be advection and diffusion caused by the same viscous interactions which control the global evolution of the nebula. The surface density of the water vapor is thus described by:

$$\frac{\partial \Sigma_{vap}}{\partial t} = \frac{3}{r} \frac{\partial}{\partial r} \left[r^{\frac{1}{2}} \frac{\partial}{\partial r} \left(\Sigma_{vap} \nu r^{\frac{1}{2}} \right) \right] + S_{vap}(r, t) \quad (11)$$

where Σ_{vap} is the surface density of water vapor, r is the distance from the sun, and $S_{vap}(r, t)$ represents the sum of the source and sink terms for the vapor at a given location and time (Stepinski and Valageas, 1996, 1997). Here, the diffusivity is assumed to be the same as the viscosity, ν , for the evolution of the nebula used in equation (1). That is, we assume a Prandtl number of 1 (Cuzzi and Zahnle, 2004). Note that in some previous studies (Stevenson and Lunine, 1988; Cyr *et al.*, 1998; Cuzzi and Zahnle, 2004), the evolution of the *concentration* of water vapor (or solids) was tracked rather than the surface density. The concentration is defined as the mass of water present relative to hydrogen (Σ_{vap}/Σ in the inner disk). Here we follow Stepinski and Valageas (1997) by explicitly tracking how the surface densities of the various water species evolve.

4.2 Dust

Dust refers to solid material that is strongly coupled to the gas ($St \ll 1$), and thus these particles are assumed to move with the gas and their motion is described by a similar equation as that which describes the motion of the water vapor:

$$\frac{\partial \Sigma_d}{\partial t} = \frac{3}{r} \frac{\partial}{\partial r} \left[r^{\frac{1}{2}} \frac{\partial}{\partial r} \left(\Sigma_d \nu r^{\frac{1}{2}} \right) \right] + S_d(r, t) \quad (12)$$

where Σ_d is the surface density of the dust. Because the dust particles are so well coupled to the gas, the diffusivity with which they are transported is again the same as the viscosity of the nebula and diffusivity of the water molecules.

4.3 Migrators

As bodies grow larger in the disk, they are still affected by the turbulence in the nebula and diffuse along concentration gradients, though to a lesser extent than dust or gas. The diffusive transport of the migrating population is described by:

$$\frac{\partial \Sigma_m}{\partial t} = \frac{3}{r} \frac{\partial}{\partial r} \left[r^{\frac{1}{2}} \frac{\partial}{\partial r} \left(\Sigma_m \nu_m r^{\frac{1}{2}} \right) \right] + S_m(r, t) \quad (13)$$

where Σ_m is the surface density of migrators and ν_m is the effective diffusivity of the migrators, given by

$$\nu_m = \frac{\nu}{1 + St} \quad (14)$$

(Cuzzi *et al.*, 1993; Cuzzi and Hogan, 2003; Cuzzi and Weidenschilling, 2005). Thus for the migrators, $\nu_m = \nu/2$.

The lower level of diffusion for these bodies is due to the fact that the migrators are not as coupled to the gas as the dust particles are. Adachi *et al.* (1976) and Weidenschilling (1977a) showed that as these bodies orbit the sun, they would experience headwinds in their orbits due to the fact that the gas in the disk rotates slower than the Keplerian rate. These headwinds caused the particles to drift inward towards the sun. In a non-uniform nebula, this same effect may cause objects to migrate outwards if local pressure maxima exist (Haghighipour and Boss, 2003). The movement of these bodies with respect to the gas is described by the mass flux equation:

$$\frac{\partial \Sigma_m}{\partial t} = -\frac{1}{r} \frac{\partial}{\partial r} (r v_{drag} \Sigma_m) \quad (15)$$

where v_{drag} is the inward migration velocity with respect to the gas. It is assumed that the migrating population moves with the maximal radial drift (which equals the difference between Keplerian velocities and the orbital velocity of the gas):

$$v_{drag} = \frac{\Delta g}{2g} V_k \quad (16)$$

where g is the acceleration due to the sun's gravity at a given location, V_k is the local Keplerian velocity, and Δg is the difference in gravitational acceleration felt by a solid object and a parcel of gas at a given location, given by:

$$\Delta g = \frac{1}{\rho_g} \frac{dP}{dr} \quad (17)$$

where dP/dr is the local pressure gradient of the nebular gas. Typically, the pressure gradient results in meter-sized bodies migrating inwards at ~ 1 AU/century, with only a weak dependence on location in the disk (Cuzzi and Weidenschilling, 2005).

An important point to stress here is that it is the Stokes number of the body which determines the category of dynamic behavior that the solid will belong to, not its size. The Stokes number is proportional to the product of the density of the object and its radius. Thus a consolidated meter-sized object will behave differently than a fluffy, meter-sized fractal because the effective densities would be very different. In the case of the fractal aggregate, the density would likely be so low that it would fall into the *dust* category ($St \ll 1$).

4.4 Planetesimals

Planetesimals (assumed to be bodies with radii of 0.5 km in our simulations) move on nearly Keplerian orbits in the nebula. While they experience a headwind similar to that of the migrating bodies, the resulting drag is not strong enough to cause them to migrate significantly due to their large inertia. Thus, we assume that the orbits of the planetesimals do not change over the course of the simulations presented here. The equation describing the evolution of the planetesimal surface density is thus simply:

$$\frac{\partial \Sigma_p}{\partial t} = S_p(r, t) \quad (18)$$

where Σ_p is the surface mass density of planetesimals and $S_p(r, t)$ is the source function of the planetesimals.

4.5 Sources and Sinks

At the same time that diffusion, migration, and advection are moving the different species around the nebula, the vapor, dust, migrators and planetesimals will be interacting with one another and their environment to transform from one species to another. Below we describe how these transformations take place and quantify the rates at which mass is exchanged between the different species that we are tracking.

4.5.1 Vaporization and Condensation

As icy solids are transported into the warm regions of the disk they will begin to vaporize. To account for this, after we solve for the temperature profile of the nebula, we can calculate the equilibrium vapor pressure, P_{eq} , for water everywhere in the nebula. If the actual vapor pressure, P_{vap} , is less than P_{eq} , and if solid ice is present, then some of the ice mass will be converted to vapor. The rate at which this will occur is given by Lichtenegger and Komle (1991):

$$Z(T) = \frac{a_1}{\sqrt{T}} e^{-\frac{a_2}{T}}, \quad (19)$$

where $a_1 = 7.08 \times 10^{31} \text{ cm}^{-2} \text{ s}^{-1} \text{ K}^{\frac{1}{2}}$ and $a_2 = 6062 \text{ K}$. The solid mass loss rate is given by:

$$\frac{dm}{dt} = -4\pi a^2 \mu m_p Z(T), \quad (20)$$

where a is the radius of the particle of interest, μ is the molecular weight of the water molecule, m_p is the mass of a proton, and k is Boltzmann's constant. In this formalism, the equilibrium vapor pressure, P_{eq} , is:

$$P_{eq} = Z(T) \sqrt{2\pi\mu m_p kT}. \quad (21)$$

We can calculate the actual water vapor pressure at the midplane through the formula:

$$P_{vap} = \frac{\Sigma_{vap}}{2H} \frac{kT}{m_{H_2O}}. \quad (22)$$

When the criteria for vaporization is met ($P_{vap} < P_{eq}$), we first convert the dust needed to vapor in order to increase P_{vap} to P_{eq} . If there is not enough dust present to do this, we then calculate the evaporation rate for the migrating bodies and convert the mass lost in a given timestep to vapor. In a timestep the change in surface density of the migrators as a result of vaporization is given by:

$$\Delta \Sigma_m^{vaporize} = \Sigma_m \frac{dm_m}{dt} \frac{\Delta t}{m_m} \quad (23)$$

with the water vapor surface density increasing by an equal but opposite amount. In this expression, Δt is the timestep taken in the model simulations. We ignore the vaporization rate of the dust particles by treating it as instantaneous because of their high surface area-to-volume ratios.

If P_{vap} is greater than P_{eq} , then water vapor will condense out of the nebula to form solid ice. In our model, we assume that excess water vapor is removed from the gas to maintain an equilibrium vapor pressure. The excess water vapor is assumed to go into the form of dust. Thus,

the excess water vapor is simply added to the dust surface density at each location in the nebula at the end of each time step. The amount of dust added at each timestep is:

$$\Delta\Sigma_d^{condense} = (P_{vap} - P_{eq})2H\frac{m_{H_2}}{kT} \quad (24)$$

and an equal amount is lost from the vapor phase.

4.5.2 Growth of Migrators

In addition to phase transitions, the solid particles will interact with one another through collisions. There are two types of collisions which we consider: accretionary and destructive. Initially, the disk is filled with dust particles from which the original generation of migrators is formed. These migrators would grow through the coagulation of dust particles. To account for this, we follow Cassen (1996) and define a parameter, t_{coag} , which is the coagulation timescale at a given location in the disk. As discussed by Cassen (1996), to make this model consistent with the findings of accretion simulations, this timescale is a function of orbital velocity and thus follows the relation:

$$t_{coag}(r) = t_{coag}(1 \text{ AU}) \frac{\Omega(1 \text{ AU})}{\Omega(r)} \quad (25)$$

We assume that in a given time interval, the surface density of new migrators will grow as:

$$\Delta\Sigma_m^{coag} = \Sigma_d \left(1 - e^{-\frac{\Delta t}{t_{coag}}}\right) \quad (26)$$

and the surface density of dust decreases by an equal amount.

The parameter, t_{coag} , represents the average timescale for migrators to grow from the local dust supply. This timescale is set by the competing effects of particle growth from collisions that arise due to brownian motion, turbulence, or differential drift and particle destruction or erosion from energetic collisions. The importance and efficiency of these processes is uncertain (Weidenschilling and Cuzzi, 1993; Weidenschilling, 1997; Dullemond and Dominik, 2005; Cuzzi and Weidenschilling, 2005). Here we assume that t_{coag} ranges from 10^3 - 10^5 years at 1 AU, consistent with timescales estimated by other authors (Cassen, 1996; Beckwith *et al.*, 2000).

In addition, if migrators already exist they can grow as they sweep up the dust particles suspended within the gas. The rate at which the surface density of the migrators grows as a result of this can be calculated as:

$$\Delta\Sigma_m^{acc} = \frac{\pi a_m^2 v_r \Sigma_d \Sigma_m}{H_d m_m} \Delta t \quad (27)$$

where v_r is the total relative velocity of the migrators with respect to the gas, m_d is the average mass of the dust particles, and H_d is the thickness of the dust layer in the nebula. We assume $H_d \sim H$ for the purposes of our modeling, meaning that little settling has taken place for the dust, due to its low Stokes number. As the migrators grow, the surface density of dust decreases by an equal amount.

4.5.3 Destruction of Migrators

While the above accounts for the collisions between the dust and the migrators, we must also account for the mutual collisions between migrators once they have formed. We assume that

when two migrators collide, they erode one another and some fraction of their mass is converted into smaller particles (thus acting as a sink for migrators and a source for dust). The collision rate can be calculated such that the surface density lost by disruption of the migrators (and gained by the dust) is given by:

$$\Delta\Sigma_m^{disrupt} = -\frac{f\pi a_m^2 \Sigma_m^2 v_t}{2H_m m_m} \Delta t \quad (28)$$

where a_m is the assumed *average* radius of the migrating particles (50 cm), v_t is the relative velocity that migrators would have with one another due to local turbulence ($v_t \sim \sqrt{\alpha}c_s$), m_m is the average mass of a migrating particle, f is an efficiency factor, and H_m is the thickness of the layer in which the migrators have settled in the nebula. Because the migrators have $St \sim 1$, this layer is given roughly by:

$$H_m = \sqrt{\frac{\alpha}{2}} H \quad (29)$$

The efficiency factor, f , represents the fraction of mass that is converted to dust in a collision. Benz and Asphaug (1999) showed that bodies of different sizes have characteristic strengths, q^* , that determine how they behave in a collision. The value of q^* represents the energy per unit mass needed in a collision for a given target to be broken into a number of pieces where the largest piece is half the mass of the original target ($q^* \sim 10^6$ erg/g is typical for 1 meter-sized objects). Thus, particles in a range of sizes will be produced as a result of the collisions. To account for this, we set the efficiency factor, f , such that

$$f = \begin{cases} 2 & \text{if } \frac{1}{2}v_t^2 \geq 2q^* \\ \frac{ke}{q^*} & \text{if } \frac{1}{2}v_t^2 < 2q^* \end{cases} \quad (30)$$

where $\frac{1}{2}v_t^2$ is the kinetic energy per gram of a migrator in a collision. For example, if $\frac{1}{2}v_t^2 = q^*$, the energy imparted into one of the migrators in the collision would be equal to its characteristic strength. This energy is enough to break up the migrator into pieces such that the largest remnant would be half the mass of the original body. Because of the symmetry of the collision, the bodies would each produce objects that were half the mass of their parent bodies, summing together to the mass of an original migrator. The rest of the mass is assumed to be converted into dust particles. More energetic collisions result in more of the mass being converted into dust, while less energetic collisions are less erosive. The surface density of the dust particles increases by the same amount that the surface density of the migrators decreases.

4.5.4 Growth of Planetesimals

How planetesimals formed in the solar nebula is unknown and has been debated for some time. Some suggested formation mechanisms include: formation through collisions of particles (Weidenschilling, 1984, 1997), turbulent concentration of particles (Cuzzi *et al.*, 2001), trapping of particles in eddies (Klahr and Henning, 1997), buildup of particles in pressure maxima in a non-uniform nebula (Haghighipour and Boss, 2003) and gravitational instabilities in a dust layer (Goldreich and Ward, 1973; Sekiya, 1998; Youdin and Chiang, 2004). Each of these mechanisms requires different nebular conditions in order to work (for example, some require negligible turbulence to enable settling while others require higher levels of turbulence to concentrate particles near eddies), and there is much debate which of those different conditions existed within the solar nebula. Some are formally inconsistent with the (turbulent) situation modeled here.

The goal of this work is not to prove or disprove any of these mechanisms for the formation of planetesimals, but rather to provide insight into the *effects* of planetesimal formation and of the timescale over which these objects form. Thus here we introduce the parameter t_{acc} , which is the timescale for planetesimals to form from the available solids in the nebula. We assume that the planetesimals have some birth function which describes how new planetesimals grow from the migrator population in a similar way that we account for the birth of migrators by dust coagulation, and that t_{acc} has the same radial dependence as does t_{coag} . While the birth functions of the migrators and planetesimals have similar forms, the timescales are not necessarily equal as the physical processes responsible for the formation of each type of object were probably very different. Thus t_{coag} and t_{acc} are not necessarily equal, but detailed simulations suggest that they may fall in the same range of values (Beckwith *et al.*, 2000). Like t_{coag} , only estimates of t_{acc} can be made, and thus we have investigated a wide range of possible values. The equation which describes the increase in surface density of the planetesimal population is:

$$\Delta\Sigma_p^{accretion} = \Sigma_m \left(1 - e^{-\frac{\Delta t}{t_{acc}}}\right) \quad (31)$$

Furthermore, the existing planetesimals can grow as they sweep up solids suspended in the disk, which can be an important effect once the planetesimal swarm grows in surface density. Here it is assumed that the planetesimal surface density grows through the accretion of solids suspended in the nebula such that the surface density of migrating bodies and dust lost from the nebula (and accreted onto the planetesimals) is:

$$\Delta\Sigma_m^{-,p} = -\frac{\pi a_p^2 \Delta v_{p,m} \Sigma_m \Sigma_p}{H_m m_p} \Delta t \quad (32)$$

$$\Delta\Sigma_d^{-,p} = -\frac{\pi a_p^2 \Delta v_{p,d} \Sigma_d \Sigma_p}{H_d m_p} \Delta t \quad (33)$$

and the surface density of the planetesimals increases by an equal, but opposite, amount. Here $\Delta v_{p,d}$ and $\Delta v_{p,m}$ represent the difference in rotation velocities between a Keplerian orbit and the dust and migrators in the nebula at a given location and $a_p=0.5$ km. It is assumed the dust moves with the gas, and thus, the difference in velocity between the planetesimals and dust, $\Delta v_{p,d}$, is equivalent to the difference in the orbital velocity of the planetesimals and that of the gas. Migrators do not just move with the gas, but instead move faster in their orbits, and therefore the difference in velocity between the planetesimals and migrators is $v_{drag}/2$ (Weidenschilling, 1977a).

While more detailed collisional and accretional models have been developed than those used here, they have generally focused simply on the formation of planetesimals, not necessarily the overall distribution of solids in the nebula or their movement across condensation fronts. Furthermore, they are prohibitive to run over wide ranges of space and time. Here we focus instead on the general evolution of the nebula and the water species inside it by considering the overall motions of the particular species of interest. By selective changes of parameters we show which are the most important and thus of interest for future study. More detailed treatments of the collisional destruction and accretion of the solids will be the subject of future work.

4.6 Method of Calculation

In performing the calculations above, we assume that the evolution of the solids in the disk only affects the evolution of the gas by determining the opacity of the disk. That is, there is no angular momentum or energy exchanged between the hydrogen-rich gas and the water species. Thus, we initially solve for the global evolution of the nebula, first by rewriting the viscosity, ν , as a function of Σ_g and r . This allows equation (1) to be solved by backwards-time finite-differencing. Once the surface density profile of the nebula is known for the next time step, the transport equations for each water-bearing species are solved for the same time interval, again with backward-time finite differencing. The sources and sinks of the species are then determined and the profiles are updated accordingly. Once all quantities have been determined, the equations are solved for the next time interval.

While the backwards-time differencing methods used in solving these equations are stable for any timestep, numerical problems may arise if too large a timestep is used when calculating the source and sink terms. Thus the timesteps used in these calculations never exceed half of a year, a time interval that is short compared to the coagulation and accretion timescales, as well as the timescale for significant transport of material in the nebula. The code was developed to run in parallel on the SGI Origins clusters at NASA Ames and Goddard. A single simulation took between 1000-3000 computer hours, depending on the extent of the grid needed to contain the disk.

In doing these calculations, it is critical to set appropriate boundary conditions. For the inner boundary of the nebula, we assumed that the surface density was equal to zero at the center ($r=0$) so that material would fall directly onto the star. The outer boundary of the grid was chosen such that the expanding outer edge of the disk was always contained within the grid. The density at the outer boundary of the grid was held at a fixed, negligible value (representing interstellar medium). Initially, outside of R_0 (the assumed “edge” of the disk at $t = 0$) the surface densities were set such that $\Sigma=10^{-20}$ g/cm², $\Sigma_d=4.5 \times 10^{-23}$ g/cm², $\Sigma_m=0$ g/cm², and $\Sigma_p=0$ g/cm².

5 Model Results

We have applied our model to investigate how the distribution of water evolves in protoplanetary disks exhibiting a variety of structures and evolutionary parameters. In carrying out a model run, the parameters given in Table 2 were assigned values and the model equations were solved for a period of 3 million years, which is the observed average lifetime of inner disks around solar type stars in young clusters (Haisch *et al.*, 2001). The initial disk has a surface density $\Sigma(r) = \Sigma_0 r^{-p}$, where Σ_0 is the surface density at 1 AU and the disk is truncated at R_0 . In reality, the values of these parameters are determined by the mass of the molecular cloud from which the star and disk form, as well as the initial angular momentum of the starting material. There is no way to know the values of these parameters for a disk like our own solar nebula, thus we consider a wide variety of initial conditions to investigate how different disk structures affect the evolution of the water distribution within them.

Table 3 lists the values of the parameters used for the cases whose results are shown in Figures 1-7. While the number of combinations for the different parameters is quite large, we present these seven cases in order to identify what effects the different parameters have on the evolution of the water distribution. In Figures 1 through 4, the disk is assumed to have a mass of $0.2M_\odot$.

distributed out to 40 AU. This type of disk is assumed to be similar in structure to those disks studied by Boss (2001, and others by the same author). In Figures 5 and 6, the disk is assumed to have the same mass as in the previous cases, but it is distributed initially out to 100 AU, leading to a less dense and more extended structure. In Figure 7, the disk again has the same mass, but the mass is distributed with a more shallow power law index, making the disk more massive at larger radii than in the other cases.

The various panels in Figures 1-7 plot the model results at different stages during the evolution of the disk (after 10^5 , 10^6 , 2×10^6 , and 3×10^6 years). In some cases numerical instabilities caused us to end a simulation before reaching 3 million years, and those cases and the reasons for the instabilities are identified below. It should be kept in mind that these times are model times, where $t=0$ corresponds to an arbitrary point in the evolution of the protoplanetary disk when we begin to track the physical processes outlined above. Our $t=0$ is not necessarily meant to be taken to be equal to the time of CAI formation or final collapse of the molecular cloud as it is uncertain when those events would take place in the formation of a protoplanetary disk. Instead it can be thought of as a point in time *very* early in the history of the disk evolution, $\ll 10^6$ years since cloud collapse. Below we discuss the evolution of a subset of cases we have modeled, focusing on identifying how different aspects of the water distribution are affected by changes in the model parameters. In the following section we discuss what implications these results have for the evolution of meteorite parent bodies, giant planet formation, and our understanding of protoplanetary disk structures.

5.1 Disk Mass and Physical Structure

The surface density evolution of the disks in these models are shown in panel A of each figure. In all cases, the mass of the disk decreases over time as material is transported inward by viscous interactions and is eventually accreted by the central star. In order to balance the effects of the inward mass movement, the disk expands outwards as small amounts of mass are pushed away from the star in order to conserve angular momentum. This latter effect can be seen as the disk grows larger in its radial extent.

The rate at which disk evolution takes place is determined by the viscosity of the disk. In the α -disk model used here, the viscosity is dependent on the temperature of the disk ($\nu \propto c_s H \propto c_s^2 \propto T_m$), and thus, the change in opacity due to material transport can be important. An extreme example of this is illustrated in Case 1 whose evolution is shown in Figure 1. In Panel A, a noticeable kink in the surface density distribution develops early on, indicating the location of the snow line in the disk. As migrators form in the outer disk, they are carried inwards where they vaporize as they cross the snow line. This results in a local increase in the opacity at the snow line as vapor diffuses upwards and outwards to condense forming small dust grains. This region is then less able to radiate away the energy that is created by viscous dissipation, and the temperature goes up. Thus the viscosity locally increases, leading to more rapid mass transport in this region of the disk. This local increase in opacity comes at the expense of the outer disk, where the disk is depleted in its dust. Thus the viscosity of the outer disk decreases at the same time. This leads to the interesting result that the rate of mass transport in the outer disk quickly declines in the early stages of evolution, while the inner disk continues to evolve at a rapid rate. Thus the surface density of the inner disk decreases more rapidly, while the evolution of the outer disk is essentially stalled in comparison. Ruden and Pollack (1991) also found that the decrease

in opacity of the disk would cause the evolution of the outer disk to halt before the inner disk and report cases where the surface densities of their model disks increased with distance from the central star. In our Case 1, this caused us to halt the evolution after 1.5 million years as numerical instabilities developed in the water transport equations.

This effect was reduced when dusty material was preserved in the outer disk, preventing large opacity gradients from developing. This could be achieved in two ways. In Case 2, the same disk structure was used as in Case 1, but the coagulation timescale is set to be an order of magnitude longer. This decreased the rate at which dust was removed from the disk, allowing it to provide a source of opacity throughout the lifetime of the disk. The second method is shown in Case 4, where we again use the same disk structure as Case 1, but now assume that α is greater by one order of magnitude. This higher value of α produces more energetic collisions between the migrators that form in the outer disk, resulting in more mass being transferred from migrators to dust than in the less turbulent case. More importantly, because the disk has a higher viscosity, the diffusivities of the species within it are greater. Thus as dust gets concentrated near the snow line to locally increase the opacity, the higher diffusivity acts to smooth out this concentration gradient by rapidly carrying dust outward again. Furthermore, viscous evolution is faster for higher values of α , leading to more rapid advection of dust which allows regions to be resupplied on shorter timescales.

As expected, the disks expand as mass is accreted through the disk due to the outward transport of angular momentum. The timescale over which a disk will grow due to its viscosity is given by $t_{vis} \sim R^2/\nu$, where R is the radial extent of the disk (Hartmann *et al.*, 1998). Thus, smaller disks and more viscous disks will evolve more rapidly, and this can be seen in the cases presented here. Also, the viscosity of the disks decrease over time as the disk cools due to dust coagulation and transport. The combination of these effects explains why there are differences in the evolution of the disks presented here versus the analytical models of Cuzzi *et al.* (2003) where in the case of a uniform disk viscosity the radial extent of the disk grew by a factor of 4 and decreased in mass by a factor of 40. The disks in Cuzzi *et al.* (2003) evolve to a greater degree than those shown here because the disks used here are initially larger in radial extent and have their viscosities decrease over their lifetimes. As will be discussed below, while $0.1 M_{\odot}$ remain in some of the disks shown here, the amount of solids left behind may be a much smaller fraction than was originally available. Thus, the solid inventory of a disk is not necessarily representative of the overall disk structure.

In addition to affecting the evolution of the surface density, the thermal structure of the disk will change as material is transported within it. As described above, the localized increase in opacity that occurs near the snow line will raise temperatures as radiation is more efficiently trapped. The localized enhancement of water generally reaches a maximum of ~ 5 - 10 , increasing the opacity by roughly the same factor. As the midplane temperature of the disk goes as the fourth root of the opacity, this would correspond in a midplane increase by a factor of ~ 1.5 . Thus if this opacity increase were to occur at the snow line, where the temperature was ~ 160 K, the increased opacity would cause the temperature to rise to ~ 240 K. The snow line would then migrate *outwards* to a new position where the viscous energy dissipated in the disk is balanced by the radiative energy of the disk to produce conditions where ice would again be stable. Once the opacity increase slows, the snow line then moves inward over time as the disk cools due to mass loss, thinning, and opacity decrease due to coagulation (Cassen, 1994; Davis, 2005).

5.2 Water Vapor Concentration

In all simulations shown here, the concentration of water vapor in the inner nebula increases over the canonical solar ratio during the early stages of evolution, as shown in panel E of each of the figures. In these panels, the concentration of water vapor relative to hydrogen is plotted, normalized to the canonical value ($\Sigma_{vap}/\Sigma \sim 4.5 \times 10^{-3}$ here, Krot *et al.*, 2000). The snow line in each case would correspond to the location where the vapor concentration drops immediately in these panels (that is the near-vertical line in the distribution). The early enhancements of water vapor result from the dust in the outer nebula coagulating to form rapidly drifting migrators. These migrators move into the hotter regions of the nebula and evaporate. The resulting vapor builds up just inside the snow line as illustrated by the 10^5 year snapshots. This is because the mass influx of migrators is greater than the removal rate of the water vapor by diffusion and advection. The vapor that is produced from the migrators is eventually spread throughout the inner nebula. Over time, the inward mass flux slows for two reasons. First, the production rate of the migrators in the outer nebula declines due to the decrease in the amount of source material (dust) present, and second, the probability that the migrators will be accreted by larger bodies rather than surviving their transport to the inner disk goes up over time as the planetesimal swarm grows in the outer disk. The decrease in the migrator influx then allows the water vapor to be removed from the inner disk faster than it can be resupplied, leading to a continual decrease in the concentration of water vapor present there. Much of the water vapor is advected inwards and accreted by the central star, while some of it is diffused outwards where it condenses to form ice particles which are incorporated into the planetesimals there.

An exception to this rule is Case 1 where removal of the dust in the outer disk, and its subsequent opacity and viscosity decrease, drastically slowed the large scale mass transport in the disk, resulting in the water vapor concentration constantly increasing in the inner disk. In these cases the hydrogen-rich gas from the inner disk was being removed at a faster rate than it was being resupplied. Water, on the other hand, was constantly being resupplied as migrators from everywhere in the disk continued to move inwards and dust from just beyond the snow line was carried inward with the gas. This led to the water vapor-to-hydrogen ratio continuing to increase, reaching very high levels over time.

The evolution of the water vapor described here is qualitatively similar to the different evolutionary stages identified by Cuzzi and Zahnle (2004), who also found that the inner nebula would go through a period of enhanced water vapor concentration. The maximum level of enhancement predicted was $E_0 = 2f_L/3\alpha$, where f_L was the fraction of solid mass contained within migrating bodies, which the authors estimated to be ~ 0.1 . This would lead to a value of $E_0 \sim 700$ for $\alpha = 10^{-4}$ and ~ 70 for $\alpha = 10^{-3}$. In most of our simulations, the maximum enhancement is ~ 5 - 10 for $\alpha = 10^{-4}$ and ~ 3 for $\alpha = 10^{-3}$, over an order of magnitude less than was predicted. This difference is partly due to f_L being less than 0.1 during the early stages of disk evolution (starting at levels < 0.01), though it also reaches values much greater than 0.1 at different locations in the disk as the disk evolves.

The major reason for the difference in vapor enhancement shown here and that predicted by Cuzzi and Zahnle (2004) is that here the source of the migrating material is depleted over time. Cuzzi and Zahnle (2004) assumed a steady state—that is, the region of the disk outside the snow line always contained its canonical value of water. In our model, as migrators are transported inwards, the outer nebula is depleted in material, reducing the source of the migrators

over time. This results in the inward mass flux of migrators decreasing over time, rather than being held constant. This effect causes the peak enhancement experienced by the inner nebula to be substantially lower than would be estimated in steady-state. The fact that the finite supply of material was the major factor in determining the maximum vapor enhancement, rather than the increasing likelihood of being swept up by a growing planetesimal population, was confirmed in runs where we did not allow planetesimals to form, thus removing the possibility of losing migrators to immobile objects. In these cases it was found that the maximum vapor enhancement did not change significantly from those cases presented here. However, if the Case 1 situation were to keep evolving, it would develop high water vapor enhancements.

As the influx of material from the outer disk continues to slow, the concentration of water vapor eventually decreases as diffusive redistribution begins to dominate the transport. Diffusion carries the water vapor outwards where it condenses to form dust grains. While these dust grains can then coagulate together to form migrators which will then move into the warm inner disk again where the processing is repeated, this recycling is not perfectly efficient. This is because planetesimals continue to form in the outer disk, trapping the dust and migrators, preventing some of the water that diffuses outward from returning to the inner disk. Also, the water vapor will also be advected inwards by the average flow of disk (that generated by the viscous shear that drives the disk evolution) and some of the vapor is then accreted onto the central star. These processes combine to deplete the inner disk in water vapor, causing the enhancement to decrease over time.

Not only is the excess water vapor removed from the inner disk, but diffusion works to continue to decrease the water-to-hydrogen ratio below the canonical solar value. Examples of such situations can easily be seen in Cases 3, 4, and 7. In Case 3, planetesimal formation happens on such short timescales that the influx of migrators to the inner disk is halted early during the disk evolution. As such, the inner disk experiences only a minor enhancement in its water vapor content before diffusion begins to dominate the transport. At that point the concentration of water decreases below the solar value and the inner disk is depleted by a factor of ~ 10 after nearly 2 million years of evolution.

Cases 4 and 7 also very quickly reach states where the concentration of water vapor decreases below the solar value. In these cases, α was assumed to be 10^{-3} , and thus the diffusivity was 10 times greater than in most of the other cases shown here. Thus in higher α cases, diffusion transports material much faster, resulting in a larger depletion of material. While Case 6 also had an α of 10^{-3} , it did not reach the same level of depletions that Cases 4 and 7 did. The reason for this is that coagulation proceeded more slowly in Case 6, meaning that the influx of migrators from the outer nebula did not decrease over such a short timescale. That is, the outer disk was able to produce migrators for a longer period of time, resupplying the inner disk with vapor over much more of the lifetime of the disk before allowing diffusion to become the dominant transport mechanism.

5.3 Solid Surface Density

Panels B, C, and D in Figures 1-7 show how the surface densities of the dust, migrators, and planetesimals of the disks change over time. In each disk the solids initially are distributed uniformly through the outer nebula in the form of dust. As discussed above, the dust begins to coagulate to form migrators which then are accreted to form planetesimals. Because of the rapid drift that migrators experience, a particular body may travel a large distance through the disk before it is

accreted—and in many cases, particularly during the early stages of disk evolution, it will migrate in to the hot inner regions of the disk and vaporize without being incorporated into planetesimals at all.

In all cases shown, the surface density of the dust peaks immediately outside the snow line at almost all times (the exception being the 3 million year snapshot in Case 3). This is similar to the results found by Stepinski and Valageas (1997) and Cuzzi and Zahnle (2004). The reason for this is that despite having the shortest coagulation time of anywhere in the outer disk (and therefore the most efficient dust sink), dust is resupplied to this region in a variety of ways. First, the net flow of material in a disk is inward, so dusty material from the outer nebula will be entrained in the gas and carried towards the central star. Secondly, migrators move inward due to gas drag and constantly resupply the region outside of the snow line with additional material. There, the turbulent velocities between the migrators are highest ($v_t = \sqrt{\alpha}c_s$) and the migrators have a larger volume density compared to anywhere else in the disk. This results in more frequent and destructive collisions between the migrators, generating more dust there than at any other location. Finally, water vapor that diffuses outward from the inner disk will condense to form water ice, and its concentration will be highest immediately outside the snow line.

Local minima, or dips, in the dust surface density develop in most of the cases shown. The outer edges of these dips, where there is a localized increase with dust surface density, correlate with the local maxima in the overall disk surface density. It is at these regions that the dust began to become depleted as it rapidly coagulates to form migrators, causing the disk viscosity to decrease, and as discussed previously, slows the local rate of mass transfer. As a result, the inward flow of material by advection decreases, preventing material from the outer disk from being carried inwards. In addition, outward diffusion of dust does not operate rapidly enough to resupply this region with dust from smaller heliocentric distances, which itself is advected further inwards by the large scale flow of the disk. Thus, dust was removed more rapidly than it was resupplied, resulting in a dip in the dust surface density. These effects are most readily observed in Cases 1 and 5.

While migrators are most efficiently produced where dust densities are high, their distribution in the disks shown do not mirror that of the dust. Because of gas drag, migrators are constantly flowing inwards, leading to a surface density that decreases with distance, despite the gaps that develop in the dust distribution. In some cases (most notably Case 1, but also 2, 5, and 7), local maxima or sharp changes in the slope of the migrator distribution are noticeable and correspond to local minima in the dust distribution. This is not due to the production rate of the migrators, but instead to the effect that the dust surface density has on the thermal evolution of the disk. Because the dust concentration determines the opacity of the disk, regions where dust is depleted will achieve lower temperatures and lower viscosities. This results in nebular gas “piling up” there due to the slower evolution. In addition, the midplane temperature gradient will locally decrease, leading to a localized decrease in the outward pressure gradient of the gas. It is this pressure gradient that determines the rate at which the migrators move inwards, and thus the velocity of the migrators will slow. Therefore, as migrators move inwards from the outer disk, they may be traveling at rates on the order of 1 AU/century as quoted above. However, as they enter these regions of shallower pressure gradients, their velocities decrease rapidly, resulting in a pile up of the migrators as the outer disk continues to rapidly feed that region with more rubble.

Another important result to notice is that the inner edge of the migrator surface density does not extend beyond the inner edge of the dust surface density (the snow line) by more than a few

tenths of an astronomical unit. This counters the finding by Cyr *et al.* (1998) who reported that icy boulders could exist as far inwards as 2 AU from the snow line due to the rapid rate at which they are transported. Instead, our results are in agreement with those of Supulver and Lin (2000) who found that icy bodies would vaporize shortly after crossing the snow line.

In looking at planetesimals, their growth occurs most rapidly immediately outside the snow line because the accretion timescale is shortest there (the local t_{acc} scales with orbital period), and because it is there, generally, that the largest amount of icy material passes (both inward from migrators and dust and outward by dust condensed from vapor). However, as the disk evolves, the planetesimal surface density is shaped by the evolution of the migrator distribution and the migration of the snow line.

As migrators move through the disk, they can be incorporated into planetesimals by interacting with one another to form new ones (through t_{acc}) or by being swept up by pre-existing ones. New planetesimals are most easily created close in to the central star where accretion timescales are shorter or where the surface density of migrators are highest. When a significant amount of planetesimals has already formed, the probability that migrators will pass through this swarm without being swept up decreases, meaning that the planetesimals at the outer edge of this large swarm will grow more rapidly far away from the snow line as migrators from the outer disk attempt to drift inwards. Rather than surviving all the way to the snow line, they instead continuously feed the large swarm further away.

As the snow line migrates inwards, planetesimals will still be able to form at smaller heliocentric distances. However, the surface density of planetesimals that forms there will be determined by how much solid material is available at these smaller distances. In the early stages of disk evolution, there is nothing to prevent material from constantly being carried inward to the snow line, as described above, and thus the largest planetesimal surface density corresponds to that location immediately beyond the snow line. As the disk evolves and the snow line moves inward, the flow of solids from the outer disk to the snow line is inhibited by the existing planetesimals at larger heliocentric distances. Thus in the later stages of disk evolution, the planetesimal surface density may peak at a location significantly outside the current location of the snow line. A similar result was seen by Kornet *et al.* (2004). This effect is most noticeable when planetesimal formation is rapid compared to the rate at which the snow line migrates. Thus in the slower evolving disks shown ($\alpha=10^{-4}$), the planetesimal surface density evolves as described. In those cases where $\alpha=10^{-3}$, the snow line migrates rapidly enough (and dust is transported more readily) so that the preferred location for planetesimal location is generally always immediately outside the snow line.

Planetesimal growth will determine how much water is retained in the disk at the end of its evolution. Below the parameters used in each case, Table 3 lists the initial mass of the disk, the mass at the end of the simulation, the initial mass of water contained in the disk, the mass of water contained in the planetesimals at the end of the simulation as well as the total mass of water in solid form. While it is clear that the enhancement of the inner disk and snow line region comes at the expense of the outer disk, it is also true that decoupling of solids depletes water from the disk as a whole. In all cases presented the water-to-hydrogen mass ratio remaining at the end of a simulation is lower than at the beginning. Because migrators are transported inward by gas drag faster than the advective velocity of the nebula, these objects speed ahead of the gas and move towards the sun faster than the rest of the material in the disk. This results in solid-forming species being lost from the disks more rapidly than other species. This was also found to be the case in the massive disk models of Stepinski and Valageas (1997). As a result, the amount of mass

that would be available to be incorporated into planetesimals far outside the snow line decreases over time, and the amount of material locked up in such bodies will only be a small fraction of the material that was available when the disk first formed. Higher fractions will remain if planetesimal formation is very efficient (operates on short timescales) as will be discussed below.

Finally, not only does the inward transport of migrators play a significant role in determining the distribution of the planetesimals near the snow line, but also at large heliocentric distances as well. In the outer disk, we find that the planetesimal surface density drops off rapidly at large distances, reaching negligible values at smaller heliocentric distances than the gas surface density. These results are similar to those found by Weidenschilling (2003), who found that the inward migration of bodies as they grow larger in size could produce a planetesimal swarm significantly smaller than the gaseous disk that orbited the sun. In the cases presented here, the planetesimal surface density may extend to distances that are a factor of two less than what the gaseous disk occupies.

6 Discussion and Implications

The results of the different case studies presented in the previous section demonstrate the sensitivity of the specific results to the values of the free parameters used. We cannot expect to know the precise starting conditions of the solar nebula or other disks; rather, we hope to use the general results presented here to understand different features of protoplanetary disks as well as the different stages through which our own solar system might have evolved. Below we discuss the implications our models have for such studies.

6.1 Inner Nebula and Chondritic Parent Bodies

The results of the various cases discussed show that the region of the disk interior to the snow line would have experienced fluctuations in the concentration of water vapor relative to hydrogen. The concentration may have been enhanced by as much as an order of magnitude and the overall enhancement may have lasted for a million years or more. As the influx of material from the outer nebula decreased, the inner nebula became depleted in water vapor, reaching concentrations that were less than expected under canonical nebular conditions. Because of its importance in determining the oxidation state (the so-called oxygen “fugacity”) of the gas, the water vapor concentration affected the chemistry and mineralogy of primitive materials in the inner disk. Thus, we can look at the properties of the chondritic meteorites to determine how much the oxidation state of the inner solar nebula changed and estimate the timescales on which these fluctuations took place. By doing so, we may be able to constrain the various parameters used in this model for our solar nebula.

Enhanced nebular oxygen fugacities have been invoked to explain a number of chemical and mineralogical features in chondritic meteorites. Among these (as reviewed by Krot *et al.*, 2000) are the valence state of titanium in Wark-Lovering rims around CAIs which requires a 5 order of magnitude increase in oxygen fugacity over the canonical solar value (Dyl *et al.*, 2005), observed Mo and W depletions in CAIs (3-4 orders of magnitude; Fegley and Palme, 1985), fayalite (FeO) grains in carbonaceous chondrites (3-4 orders of magnitude; Hua and Buseck, 1995), fayalitic olivine in carbonaceous and ordinary chondrite meteorites (2-4 orders of magnitude;

Palme and Fegley, 1990), FeO content in chondrules (4-6 orders of magnitude; Huang *et al.*, 1996; Hewins, 1997), and retention of volatiles during formation of FeO rich chondrules (2-5 orders of magnitude; Yu and Hewins, 1998). In the model cases presented here, the maximum enhancement produced was no more than one order of magnitude, suggesting that enhanced oxygen fugacities of the type needed to produce the observed signatures in meteorites cannot be produced by the radial transport of water alone.

While this is true in the specific cases presented here, we can also calculate whether this limited enhancement is true for all disks. The enhanced water vapor concentration of the inner disk will result from water ice from the outer disk being brought inside of the snow line where it would vaporize. Thus the maximum possible enhancement will be achieved when all of the water in the disk is concentrated inside of the snow line. If the concentration of water relative to hydrogen is initially some constant fraction throughout the disk, then the maximum enhancement possible will go roughly as the mass of the disk divided by the mass of the disk interior to the snow line. The amount of mass in a disk inside a given radius, R , whose surface density is described as a power law (as is assumed here) is:

$$M_D(r < R) = \frac{2\pi r_0^p \Sigma_0}{2-p} R^{2-p}, \quad (34)$$

where r_0 is 1.5×10^{13} cm (1 AU, where Σ_0 is defined). Thus, initially the ratio of the amount of mass in the disk to the amount inside the snow line will be $(R_0/R_{sl})^{2-p}$. As an example, this formula predicts that the maximum enhancement possible in case 2 would be 40 AU/5 AU ~ 8 for $p = 1$, which is close to the value found in the model runs with $t_{coag} \sim 10^4$ years. In order to enhance the inner solar nebula with water vapor by just 3 orders of magnitude (roughly the lower level needed to produce some of the oxidized features of meteorites identified above) requires that the disk extended outwards to ~ 5000 AU (for $p = 1$) if the snow line were located at 5 AU. Smaller disks would be needed if the surface density distribution had a slope of $p < 1$, so that most of the disk mass was concentrated at larger radii. In the unlikely case of $p = 0$, which would represent a disk with a constant surface density at all radii, the disk would have to extend to 160 AU to enrich the inner disk by 3 orders of magnitude. More plausible disk structures with $R_0 \sim 50 - 200$ AU, $p \sim 1$ and $R_{sl} \sim 2 - 10$ AU predict enhancements of 5-100. However, it must be remembered that these are *maximum* values as these calculations assume that no water would be left beyond the snow line. Transporting all water in the disk to inside the snow line is likely not feasible, however, and thus in real disks, it is unlikely that the maximum enhancements would be reached. Our findings suggest that the maximum enhancement of water vapor a real disk would experience is roughly an order of magnitude.

The large oxygen fugacities recorded by some chondritic meteorites thus are likely not due to the inward migration of icy bodies alone. In reviewing the different features, Krot *et al.* (2000) argued that many could have resulted from asteroidal processing as primitive materials reacted with oxidizing fluids (liquid water) after they were accreted by their parent bodies. However, nebular processes may have still played a role as the enhanced water vapor concentration would lead to a more oxidizing nebular gas that could combine with other processes that would concentrate silicate dust to enhance the oxygen fugacity in the inner disk, provided that there was a way to vaporize the dust, perhaps in a chondrule forming event.

The enhancement of water vapor in a chondrule formation event was considered by Ciesla *et al.* (2003) who demonstrated that if shock waves, such as the type thought to be responsible for the

formation of chondrules, occurred in an icy region of the solar nebula, large water vapor pressures could result. The shock wave alone would increase the vapor pressure by almost two orders of magnitude, though hydrogen would increase by an equal amount, maintaining a constant *concentration*, and thus keeping the oxygen fugacity roughly the same as it was before the shock occurred. However, the higher partial pressures of all vapor species would create a new, temporary environment which may then allow chemistry to proceed along different paths or rates than it would under the pre-shock conditions. If the shock waves were to occur in regions of the disk where solids were concentrated above the solar value, then those solids may be vaporized, releasing the oxygen they contained to the gas. Regions of a disk that are enhanced in solids can be caused by gravitational settling to the disk midplane (Weidenschilling, 1980) or by turbulent concentration (Cuzzi *et al.*, 2001), with enhancements exceeding 100 times solar predicted to be common. If these solids are vaporized, vapor pressures 10^4 - 10^5 larger than found in the canonical nebula would be possible, if combined with global enhancements due to the inward migration of water as described above. In fact, Dyl *et al.* (2005) argue that the Ti oxidation states that they observe in the Wark-Lovering rims of CAIs are likely due to shock waves in a dusty gas. Further work is needed to confirm that such temporary environments could imprint their signatures on the various primitive materials described above.

While some chondritic meteorites appear to have formed in regions of the nebula with higher-than-solar oxygen fugacities, others appear to have formed in environments that were more reducing than canonical conditions. Models for the formation of the enstatite chondrites suggest that removal of more than 50% of the water in the nebula had to have taken place in order for the observed minerals to become stable (Hutson and Ruzicka, 2000; Pasek *et al.*, 2005). Such a situation is realized in the model runs presented here, but after millions of years of evolution. In order for water to be depleted so that its concentration is low enough to allow the enstatite mineralogy to be reproduced, either the disk has to have a large enough viscosity ($\alpha > 10^{-4}$) to ensure that vapor can diffuse outwards rapidly enough, or meter-sized rubble must be prevented from reaching the inner disk. Neither of these situations would allow for the inner disk to become substantially *enhanced* in vapor as well. Thus it may be that large water vapor enhancements throughout the region interior to the snow line followed by large depletions are difficult to get in the same protoplanetary disk.

In addition to the different oxygen fugacities recorded by primitive meteorites and their components, different oxygen isotope abundances are also observed. On an oxygen three-isotope plot, CAIs and chondrules fall on a line with a slope of ~ 1 , which has been interpreted to arise due to the mixing of an ^{16}O rich gas with a reservoir rich in ^{17}O and ^{18}O (Clayton, 1993). It has been suggested that this mixing may have arisen as the inner nebula gas, which was ^{16}O rich, incorporated the water vapor that was introduced by inwardly migrating water-ice boulders which were ^{16}O -poor. The excess heavy oxygen isotopes in these boulders could be due to isotopic self-shielding during CO dissociation in the parent molecular cloud of the solar nebula (Yurimoto and Kuramoto, 2004) or the outer disk (Lyons and Young, 2005). Either mechanism requires the inward drift and evaporation of outer solar system rubble to alter the oxygen isotope ratio of inner disk solids (Yurimoto and Kuramoto, 2004; Lyons and Young, 2005; Krot *et al.*, 2005). Krot *et al.* (2005) reported on one CAI which formed in an ^{16}O -poor environment with an age of less than 0.8 Myr, suggesting that icy material would have to be brought inwards rapidly in order to alter the gaseous isotopic abundances in the nebula. (This age was determined assuming that ^{26}Al was uniformly distributed in the disk and was not altered by later injection or

local production of the nuclide.) In the model developed here, enough ice was introduced to the inner nebula in less than 0.1 Myr that the region immediately inside the snow line would reach its maximum enhancement. Over the next few hundred thousand years, the rest of the inner nebula would be equally enhanced and its isotope abundances would be modified. Even small enhancements of the inner nebula can lead to large changes in the oxygen isotope abundances (Yurimoto and Kuramoto, 2004), and thus determining how much outer-nebula water ice must be brought inwards to produce the observed isotopic trends could provide a constraint on the level of mixing that took place in the solar nebula.

6.2 Implications for Giant Planet Cores

One of the motivations for previous studies of the distribution of water in the solar nebula was to evaluate if water would be concentrated at a location that would allow rapid growth of large bodies which would become the cores of the giant planets (assuming they grew through the core accretion mechanism). Stevenson and Lunine (1988) showed that significant concentrations were possible immediately beyond the snow line due to the outward diffusion of water vapor alone, but they neglected the migration of bodies from the outer nebula. Stepinski and Valageas (1997) developed a more detailed model which considered the evolving distribution of water throughout a protoplanetary disk and also concluded that the surface density of icy planetesimals would peak immediately outside of the snow line. From this, they argued that the largest icy body (or planet with the largest icy core) would form at this location. Cuzzi and Zahnle (2004) noted that evaporation front effects produced a larger enhancement than inward migration of solids or outward diffusion of vapor alone, however the enhancements found there were larger than those found here because of the assumption of a steady-state.

In some of the cases presented here, a similar result was observed, though, the largest surface density of icy planetesimals was not always located immediately outside of the contemporary snow line. This is due to the fact that the location of the snow line migrates inwards over the lifetime of the disk as a result of the decrease in internal heating and optical thickness of the disk. During the early stages of disk evolution, icy planetesimal formation would occur only in the outer regions of the nebula. As the snow line migrates inwards, icy planetesimals could grow at smaller heliocentric distances. If planetesimal formation occurred rapidly enough, a massive planetesimal swarm could develop near the initial location of the snow line. As migrators move inwards from the outer nebula, they continue to feed *this* planetesimal swarm because the planetesimals have a large accretional cross-section. Very few of the migrators would survive passing through this region, so the raw material that would be needed to build planetesimals at later times closer to the sun would be limited to what was already there or what was brought outwards from the vapor in the inner disk. Thus, the peak in the icy planetesimal surface density may “remember” the snow line of earlier stages of nebular evolution (c.f. Kornet *et al.*, 2004). Our results indeed show a relatively *broad* distribution of planetesimals. This may have implications for the formation of multiple gas giant cores in close proximity (Thommes *et al.*, 1999).

Another effect of solid transport is the feedback onto the viscosity of the disk. Previous studies neglected how the opacity throughout the disk would change as the dust concentration evolved. In some cases, the pressure gradient of the disk may be altered to slow the rate at which solids would drift inward due to gas drag. This would result in a traffic jam of particles as they were forced to suddenly slow down, leading to a localized region of high solid mass

density. This could be a preferred location for the formation of planetesimals or larger bodies. This is slightly different from the results of Haghighipour and Boss (2003) who found that solids would drift to and concentrate at local pressure maxima in a protoplanetary disk. In this work, no pressure maximum exists; instead, it is a shallow pressure gradient that encourages the spatial concentration of solids.

Finally, as dust coagulated to form larger bodies in the outer disk, or were removed from the region entirely, temperatures would decrease due to the lower opacity. This would produce much cooler temperatures in the outer disk than would be predicted in models where the opacity is determined as if solids were at their solar concentration relative to hydrogen. As a result, this may play a role in determining how far inward noble gases could be incorporated into solids. As reviewed by Owen *et al.* (1999), the noble gas content of Jupiter suggests that the planet incorporated a number of planetesimals that formed at very low temperatures (~ 30 K). If the opacity of the outer disk dropped rapidly enough, this may allow such temperatures to form much closer to Jupiter than the 30 AU predicted by Owen *et al.* (1999). This is speculative and requires a better treatment of disk opacity than used here.

6.3 Implications for the Structure of Protoplanetary Disks

One striking result in all cases studied is how quickly the concentration of water in the nebula deviates from the canonical value at all locations. Typically the distribution of solids (or of any chemical species in the gas phase) in models of the solar nebula or a protoplanetary disk is assumed to be a constant. Here we find that because solids are transported through a disk at different rates depending on their sizes, the abundance of a species—in both its vapor and solid phases—will vary with both time and location in the disk. This must be considered when interpreting observations of disks around young stars. For example, to infer the mass of a disk, observations will measure the solids with the greatest opacity (the dust). As can be seen in the various panel B's shown in these simulations, the shape of the dust distribution and its abundance relative to the gas can vary greatly. In addition, because solid-forming species are preferentially lost from the outer nebulae due to the inward migration of meter-sized rubble, disks at 10-100 AU likely contain more hydrogen and helium than are inferred by assuming a constant ratio of solids to gas. Therefore the masses of protoplanetary disks that have been inferred based on observations could be underestimates of the actual masses, and perhaps the sizes as well.

Decoupling of solids and gas should also be considered when trying to reconstruct the structure of the solar nebula from the solids currently present in the solar nebula. Weidenschilling (1977b) and Hayashi (1981) calculated the structure of a “Minimum Mass Solar Nebula,” where the planetary material currently in orbit around the sun was distributed into annuli around the sun to represent where the material was accreted from. The amount of hydrogen and helium needed in order to reproduce the canonical solar abundance ratio of this material at each radius was then calculated, and from that, the surface density of the nebula was found. In the calculations presented here, the planetesimal surface densities did not follow the same structure as the gas (compare panels A to D in all cases shown). If enough hydrogen and helium were added at every location to reproduce the canonical water-to-hydrogen mass ratio based on the planetesimal surface densities, the resulting nebula would have a very different radial structure and overall mass than those actually calculated in the model. Because solid-building species are lost from the disk faster than the hydrogen and helium gas, the solar nebula was likely more massive and extended to larger

radii than the minimum mass nebula estimates.

Another result of this model is that the material which is accreted onto the central star will vary in its chemical composition over time. In the models presented here, the amount of water at the very inner edge of the disk was initially equal to the canonical amount expected. As the inner disk became enhanced in water vapor, the central star would accrete more water than under canonical conditions. Later, as the concentration of water decreased in the inner nebula, the amount of water accreted by the central star would be below the canonical ratio. Carr *et al.* (2004) reported that observations of hot molecular H₂O and CO vapor inside of 0.3 AU around the young stellar object CSVS 13 indicate that the abundance of water is 10 times lower than chemical equilibrium models predict. This could result from water being depleted in the inner nebula as it is locked up in immobile objects further away as illustrated in the later stages of the models presented here, or that excess CO is being introduced into the vapor as refractory C-containing solids migrate inwards (Cuzzi *et al.*, 2003). The varying chemical abundances of accreting material may also have implications for determining the metallicity of stars, if the accreted material is concentrated in the surface layers of the star and not well mixed.

7 Summary and Discussion

In this paper we have developed a model to track the evolution of water in a turbulently evolving protoplanetary disk. Such a disk is capable of explaining the mass transport observed to take place in protoplanetary disks as well as expected to have occurred in our own solar nebula. We find that the transport of material in an evolving disk can lead to large enhancements and depletions of a chemical species that vary with time and location. This is a natural, unavoidable, result of disk evolution, and these abundance variations may be able to explain some of the observed properties of primitive meteorites, giant planets, and protoplanetary disks. In particular, transport would lead to fluctuating oxidation and isotopic conditions inside the snow line which are thought to be reflected in various components of chondritic meteorites. In addition, the changes in the distribution of solids in the disk will cause opacity variations that will change the thermal and pressure structure of the disk. This could help lead to the spatial concentration of particles in the outer disk, possibly aiding in the rapid formation of giant planet cores.

The results of the model developed here qualitatively agree with those of the previous studies reviewed earlier. The concentration of water vapor in the inner disk is expected to change throughout the lifetime of the disk, as it is enhanced during the early stages of evolution and then declines to sub-solar values at later stages. Solids preferentially concentrate immediately outside the snow line of the disk as growth processes operate on shorter timescales there than at larger heliocentric distances and transport processes continue to feed that area with raw materials to grow larger objects. Because solids decouple from the gas as they grow larger, their distribution in a protoplanetary disk can vary greatly from the distribution of hydrogen and helium which dominate the mass of the disk. Finally, the mass of solids retained in a disk is higher for more extended disks as the greater distances over which they would be transported provide more opportunity to be accreted into immobile objects. For instance, future studies should explore larger disks, as large as perhaps 200-300 AU.

While these general results agree with previous work, there are differences in our results due to the different assumptions and treatments used in this model. While the water vapor concentration

will be enhanced in the inner disk, the finite supply and rate of transport of ice to the inner disk limits this enhancement to be no more than a factor of ~ 10 , though there is no limit to the level of depletion for the inner disk. Also, the transport and coagulation of the dust particles, which determine the opacity of the disk, has a feedback effect on the evolution of the overall disk surface density. The temperature structure of the disk would also be affected, leading to sharp radial variations in the rate of both gas and solid transport. Finally, because the different dynamic categories of solids are tracked simultaneously rather than assuming a single size of objects at a given radius, it is found that the planetesimal surface density distribution is controlled by both the accretion rate and rate at which the disk cools resulting in the snow line migrating inwards. The peak in planetesimal surface density may exist well outside the snow line in the later stages of disk evolution if the accretion timescale is short compared to the cooling timescale. This may help us explain the presence of water well inside the orbit of Jupiter.

Even though this paper has focused on the dynamical behavior of water, the results can be extended to other substances in protoplanetary disks such as silicates or organics. Because both of these materials vaporize at higher temperatures than water, their respective evaporation fronts would be located much closer to the central star than the snow line. This would lead to higher levels of enhancement in the vapor phase for each species as the vapor would be distributed over a smaller area in the disk (Cuzzi *et al.*, 2003). Also, the enhanced vapor would last for a shorter period of time as the accretional timescales would be shorter at the smaller heliocentric distances, leading to a more rapid growth of the planetesimal swarm outside of the evaporation front.

The above discussion assumes that the migrators are pure substances, that is they are only made of silicates, organics, or in the model presented here, water ice. In reality, solar nebula solids were likely a mixture of all solids available at the locations that they formed and accreted. Thus the migrators may not release vapor as readily as found in this work, for example if a silicate crust were to form on the surface of the bodies preventing the release of water to the gas. This may result in water surviving in particles further inside the snowline than found here. However, collisions with other objects expose buried ice, minimizing this effect. More work is needed to understand how bodies of mixed composition can survive transport into different thermal environments.

One result that stands out from this work is the fact that there was an intimate connection between the chemical evolution of the inner disk and the physical processes in the disk. The chemical inventory of the inner disk will be determined in part by the addition of material from the outer disk or removal of material by outward diffusion. The efficiency of these processes will be determined by the growth rate of solids in the outer disk and the processes in the disk that would determine how they are transported. This means that constraints on outer disk processes may be recognized by studying primitive meteorites. For example, determining the time over which meteoritic components with different oxidation states formed could provide information on when large bodies in the outer solar system began to form. Likewise, by understanding the variations in oxygen isotope ratios we may be able to constrain the level of mixing which took place between the inner and outer solar nebula.

While this work provides insight into the dynamical behavior of water in an evolving protoplanetary disk, it can be improved in a number of ways by including more detailed considerations of the physical processes discussed. The simplifications made here were generally done in order to ease the computational burden of the model. One of the fundamental issues that requires more work is understanding the details of what drives protoplanetary disk evolution. The benefit of

the α -disk model used here is that it allows us to calculate how a disk evolves over millions of years; however there is still much debate as to what the proper value of α is and whether the model is a truly valid parametrization of what drives the disk evolution. In this work, and in most other models, α is assumed to be spatially and temporally constant, despite the fact that we are unsure of what determines its value. If the turbulence in the disk is due to the magnetorotational instability (Balbus and Hawley, 1991), then turbulence may be limited to those regions of the disk where the ionization of the gas was above some critical value. This could lead to spatially heterogeneous turbulence, where the very inner and outer parts of the disk were active while the region from ~ 1 -10 AU would be nearly dead (Gammie 1996, see however Fleming and Stone, 2003). If $\alpha \sim 0$ near the snow line, the vapor that is produced from the migrators would pile up immediately inside of the snowline could reach enhancements well above the order of magnitude found here, though over only a narrow radial band. Similarly, if the viscosity of the inner disk exceeded that of the outer disk (either due to higher α or the opacity effects illustrated by Case 1), hydrogen gas could be preferentially removed faster than the water is delivered to the inner disk, resulting again in higher water-to-hydrogen ratios than predicted here. There are mechanisms other than the magnetorotational instability that may have played a role in driving disk evolution which may have all played a role at different times and locations in the disk (Stone *et al.*, 2000). It is also possible that once larger bodies grow in the outer disk, they may excite waves that will generate or increase the turbulence in the disk (Estrada and Mosqueira, 2004; Boley *et al.*, 2005).

In terms of the evolution of the solids, we have only accounted for particle growth in the timescale formalisms described in Section 4. In reality, particle growth in a protoplanetary disk is a difficult problem that we are still trying to understand. We are unsure how fine-grained dust particles coagulate together to form large, coherent objects rather than simple dustball structures of loosely bound monomers. These individual grains and aggregates likely encountered each other at a range of velocities, some of which were accretional and others that were destructive. Models of these processes tend to focus on looking at how these objects grow at a single location in the disk, investigating the vertical distribution and settling of the solids (e.g. Weidenschilling, 1997; Dullemond and Dominik, 2005). The disk-wide radial transport of objects, and the local solid enhancements and depletions of material that we have shown here to occur, are neglected. Again, the computational rigor of such models prevent calculations of full-scale disk evolution. However, these models are critical to determining how particle growth occurs in disks under a variety of conditions. These will prove useful in constraining not only the timescales used in this model, but also allow investigation of possible delays in the initiation of planetesimal formation, for instance, which may only be able to occur once a certain physical situation (e.g. low turbulent velocities or large concentration of solids) is realized. An initial delay in planetesimal formation may lead to slightly larger vapor enhancements in the inner disk, and then once the formation process begins, allow for the rapid depletion of vapor as sites for the sequestering of water in the outer disk grow.

Finally, while more numerical modeling is clearly needed to evaluate the robustness of the assumptions made and to constrain the free parameters used in this work, further constraints and insights may be gained from studies of primitive meteorites. Radiometric dating may help set the accretional timescale for meteorite parent bodies or identify the timescale over which the chemical environment in the solar nebula changed. Also, astronomical observations of protoplanetary disks that are able to map different chemical species (i.e. dust versus gas or H₂O versus CO) will show how the distribution of various species differ and how they are separated by disk dynamics.

Indeed, measurements of these different objects will provide the needed data to which model predictions can be compared.

Acknowledgements

FJC was supported by the National Research Council while this work was done. JNC was supported by the Origins of Solar System program and the Planetary Geology & Geophysics program. Conversations with Paul Estrada, Sanford Davis, Sasha Krot, and Misha Petaev were immensely beneficial and appreciated. We are also grateful for the detailed reviews by Tomasz Stepinski and Joseph Nuth III which led to a much improved manuscript.

References

- Adachi, I., Hayashi, C., and Nakazawa, K., 1976. The gas drag effect on the elliptical motion of a solid body in the primordial solar nebula. *Prog. Theor. Phys.* 56, 1756–1771.
- Balbus, S. A. and Hawley, J. F., 1991. A powerful local shear instability in weakly magnetized disks. I - Linear analysis. II - Nonlinear evolution. *Astrophys. J.* 376, 214–233.
- Beckwith, S. V. W., Henning, T., and Nakagawa, Y., 2000. Dust properties and assembly of large particles in protoplanetary disks. In Mannings, V., Boss, A. P., and Russell, S. S. (Eds.) *Protostars and Planets IV*, Univ. of Arizona Press, Tucson. pp. 533-558.
- Benz, W. and Asphaug, E., 1999. Catastrophic disruptions revisited. *Icarus* 142, 5–20.
- Boley, A. C., Durisen, R. H., and Pickett, M. K., 2005. The three-dimensionality of spiral shocks in disks: did chondrules catch a breaking wave? In Krot, A. N., Scott, E. R. D., and Reipurth, B., (Eds.) *Chondrites and the Protoplanetary Disk*, A. S. of the Pacific Conference Series vol. 341. pp. 839–848.
- Boss, A. P., 2001. Gas giant protoplanet formation: disk instability models with thermodynamics and radiative transfer. *Astrophys. J.* 563, 367–373.
- Boss, A. P., 2004. Evolution of the solar nebula. VI. Mixing and transport of isotopic heterogeneity. *Astrophys. J.* 616, 1265–1277.
- Calvet, N., Hartmann, L., and Strom, S. E., 2000. Evolution of disk accretion. In Mannings, V., Boss, A. P., and Russell, S. S. (Eds.) *Protostars and Planets IV*, Univ. of Arizona Press, Tucson. pp. 377–400.
- Calvet, N., Briceño, C., Hernández, J., Hoyer, S., Hartmann, L., Sicilia-Aguilar, A., Megeath, S. T., and D’Alessio, P., 2005) Disk evolution in the Orion OB1 association. *Astron. J.* 129, 935–946.
- Carr, J. S., Tokunaga, A. T., and Najita, J., 2004. Hot H₂O emission and evidence for turbulence in the disk of a young star. *Astrophys. J.* 603, 213–220.
- Cassen, P., 1994. Utilitarian models of the solar nebula. *Icarus* 112, 405–429.

- Cassen, P., 1996. Models for the fractionation of moderately volatile elements in the solar nebula. *Meteorit. Planet. Sci.* 31, 793–806.
- Ciesla, F. J., Lauretta, D. S., Cohen, B. A., and Hood, L. L., 2003. A nebular origin for chondritic fine-grained phyllosilicates. *Science* 299, 549–552.
- Clayton, R. N., 1993. Oxygen isotopes in meteorites. *Annu. Rev. Earth Pl. Sc.* 21, 115–149.
- Cuzzi, J. N. and Hogan, R. C., 2003. Blowing in the wind I. Velocities of chondrule-sized particles in a turbulent protoplanetary nebula. *Icarus* 164, 127–138.
- Cuzzi, J. N. and Weidenschilling, S. J., 2005. Particle-gas dynamics and primary accretion. In Lauretta, D. S. and McSween, H. Y., (Eds.) *Meteorites and the Early Solar System II*, In Press.
- Cuzzi, J. N. and Zahnle, K. J., 2004. Material enhancement in protoplanetary nebulae by particle drift through evaporation fronts. *Astrophys. J.* 614.
- Cuzzi, J. N., Dobrovolskis, A. R., and Champney, J. M., 1993. Particle-gas dynamics in the midplane of a protoplanetary nebula. *Icarus* 106, 102–134.
- Cuzzi, J. N., Hogan, R. C., Paque, J. M., and Dobrovolskis, A. R., 2001. Size-selective Concentration of Chondrules and Other Small Particles in Protoplanetary Nebula Turbulence. *Astrophys. J.* 546, 496–508.
- Cuzzi, J. N., Davis, S. S., and Dobrovolskis, A. R., 2003. Blowing in the wind. II. Creation and redistribution of refractory inclusions in a turbulent protoplanetary nebula. *Icarus* 166, 385–402.
- Cuzzi, J. N., Ciesla, F. J., Petaev, M., Krot, A. N., Scott, E. R. D., and Weidenschilling, S. J., 2004. History of thermally processed solids in the protoplanetary disk: reconciling theoretical models and meteoritical evidence. In Krot, A. N., Scott, E. R. D., and Reipurth, B., (Eds.) *Workshop on Chondrites and the Protoplanetary Disk*, A. S. of the Pacific Conference Series vol. 341. pp. 732–773.
- Cyr, K. E., Sears, W. D., and Lunine, J. I., 1998. Distribution and evolution of water ice in the solar nebula: implications for solar system body formation. *Icarus* 135, 537–548.
- Davis, S. S., 2003. A simplified model for an evolving protoplanetary nebula. *Astrophys. J.* 592, 1193–1200.
- Davis, S. S. (2005). Condensation front migration in a protoplanetary nebula. *Astrophys. J.* 620, 994–1001.
- Dullemond, C. P. and Dominik, C. (2005). Dust coagulation in protoplanetary disks: A rapid depletion of small grains. *Astron. Astrophys.* 434, 971–986.
- Dyl, K. A., Simon, J. I., Russell, S. S., and Young, E. D., 2005. Rapidly changing oxygen fugacity in the early solar nebula recorded by CAI rims (abstract). 36th Annual Lunar and Planetary Science Conference, # 1531.

- Estrada, P. R. and Mosqueira, I., 2004. On the final mass of giant planets. In Lunar and Planetary Institute Conference Abstracts, # 1854.
- Fegley, B. and Palme, H., 1985. Evidence for oxidizing conditions in the solar nebula from MO and W depletions in refractory inclusions in carbonaceous chondrites. *Earth Planet. Sci. Let.* 72, 311–326.
- Fleming, T. and Stone, J. M. 2003. Local magnetohydrodynamic models of layered accretion disks. *Astrophys. J.* 585, 908–920.
- Gail, H.-P., 2001. Radial mixing in protoplanetary accretion disks. I. Stationary disc models with annealing and carbon combustion. *Astron. Astrophys.* 378, 192–213.
- Gammie, C. F., 1996. Layered accretion in T Tauri disks. *Astrophys. J.* 457, 355–362.
- Goldreich, P. and Ward, W. R., 1973. The formation of planetesimals. *Astrophys. J.* 183, 1051–1062.
- Haghighipour, N. and Boss, A. P., 2003. On gas drag-induced rapid migration of solids in a nonuniform solar nebula. *Astrophys. J.* 598, 1301–1311.
- Haisch, K. E., Lada, E. A., and Lada, C. J., 2001. Disk frequencies and lifetimes in young clusters. *Astrophys. J.* 553, L153–L156.
- Hartmann, L., Calvet, N., Gullbring, E., and D’Alessio, P., 1998. Accretion and the evolution of T Tauri disks. *Astrophys. J.* 495, 385–400.
- Hayashi, C., 1981. Structure of the solar nebula, growth and decay of magnetic fields and effects of magnetic and turbulent viscosities on the nebula. *Prog. Theor. Phys. Supp.* 70, 35–53.
- Hersant, F., Gautier, D., and Huré, J., 2001. A Two-dimensional model for the primordial nebula constrained by D/H measurements in the solar system: implications for the formation of giant planets. *Astrophys. J.* 554, 391–407.
- Hester, J. J. and Desch, S. J., 2005. Understanding our origins: Star formation in H II region environments. In Krot, A. N., Scott, E. R. D., and Reipurth, B., (Eds.) *Workshop on Chondrites and the Protoplanetary Disk*, A. S. of the Pacific Conference Series vol. 341. pp. 131–144.
- Hewins, R. H., 1997. Chondrules. *Annu. Rev. Earth Pl. Sc.* 25, 61–83.
- Hua, X. and Buseck, P. R., 1995. Fayalite in the Kaba and Mokoia carbonaceous chondrites. *Geochim. Cosmochim. Acta* 59, 563–578.
- Huang, S., Lu, J., Prinz, M., Weisberg, M. K., Benoit, P. H., and Sears, D. W. G., 1996. Chondrules: their diversity and the role of open-system processes during Their Formation. *Icarus* 122, 316–346.
- Huré, J.-M., Richard, D., and Zahn, J.-P., 2001. Accretion discs models with the β -viscosity prescription derived from laboratory experiments. *Astron. Astrophys.* 367, 1087–1094.

- Hutson, M. and Ruzicka, A., 2000. A multi-step model for the origin of E3 (enstatite) chondrites. *Meteorit. Planet. Sci.* 35, 601–608.
- Keller, C. and Gail, H.-P. 2004. Radial mixing in protoplanetary accretion disks. VI. Mixing by large-scale radial flows. *Astron. Astrophys.* 415, 1177–1185.
- Klahr, H. H. and Henning, T., 1997. Particle-trapping eddies in protoplanetary accretion disks. *Icarus* 128, 213–229.
- Kornet, K., Róžyczka, M., and Stepinski, T. F., 2004. An alternative look at the snowline in protoplanetary disks. *Astron. Astrophys.* 417, 151–158.
- Krot, A. N., Fegley, B., Lodders, K., and Palme, H., 2000. Meteoritical and astrophysical constraints on the oxidation state of the solar nebula. In Mannings, V., Boss, A. P., and Russell, S. S. (Eds.) *Protostars and Planets IV*, Univ. of Arizona Press, Tucson. pp. 1019–1054.
- Krot, A. N., Hutcheon, I. D., Yurimoto, H., Cuzzi, J. N., McKeegan, K. D., Scott, E. R. D., Libourel, G., Chaussidon, M., Aléon, J., and Petaev, M. I., 2005. Evolution of oxygen isotopic composition in the inner solar nebula. *Astrophys. J.* 622, 1333–1342.
- Laughlin, G. and Rozyczka, M., 1996. The effect of gravitational instabilities on protostellar disks. *Astrophys. J.* 456, 279–291.
- Lichtenegger, H. I. M. and Komle, N. I., 1991. Heating and evaporation of icy particles in the vicinity of comets. *Icarus* 90, 319–325.
- Lin, D. N. C. and Papaloizou, J., 1985. On the dynamical origin of the solar system. In D. C. Black and M. S. Matthews, (Eds.), *Protostars and Planets II*, Univ. of Arizona Press, Tucson, pp. 981–1072.
- Lyons, J. R. and Young, E. D., 2005. CO self-shielding as the origin of oxygen isotope anomalies in the early solar nebula. *Nature* 435, 317–320.
- Mathis, J. S., Rumpl, W., and Nordsieck, K. H., 1977. The size distribution of interstellar grains. *Astrophys. J.* 217, 425–433.
- Meakin, P. and Donn, B., 1988. Aerodynamic properties of fractal grains - Implications for the primordial solar nebula. *Astrophys. J.* 329, L39–L41.
- Miyake, K. and Nakagawa, Y., 1993. Effects of particle size distribution on opacity curves of protoplanetary disks around T Tauri stars. *Icarus* 106, 20–41.
- Morfill, G. E. and Völk, H. J., 1984. Transport of dust and vapor and chemical fractionation in the early protosolar cloud. *Astrophys. J.* 287, 371–395.
- Owen, T., Mahaffy, P., Niemann, H. B., Atreya, S., Donahue, T., Bar-Nun, A., and de Pater, I., 1999. A low-temperature origin for the planetesimals that formed Jupiter. *Nature* 402, 269–270.

- Palme, H. and Fegley, B. J., 1990. High-temperature condensation of iron-rich olivine in the solar nebula. *Earth Planet. Sci. Let.* 101, 180–195.
- Pasek, M. A., Milsom, J. A., Ciesla, F. J., Lauretta, D. S., Sharp, C. M., and Lunine, J. I., 2005. Sulfur chemistry with time-varying oxygen abundance during Solar System formation. *Icarus* 175, 1–14.
- Pollack, J. B., Hollenbach, D., Beckwith, S., Simonelli, D. P., Roush, T., and Fong, W., 1994. Composition and radiative properties of grains in molecular clouds and accretion disks. *Astrophys. J.* 421, 615–639.
- Pringle, J. E., 1981. Accretion discs in astrophysics. *Annu. Rev. Astron. Astr.* 19, 137–162.
- Richard, D. and Davis, S. S., 2004. A note on transition, turbulent length scales and transport in differentially rotating flows. *Astron. Astrophys.* 416, 825–827.
- Richard, D. and Zahn, J.-P., 1999. Turbulence in differentially rotating flows. What can be learned from the Couette-Taylor experiment. *Astron. Astrophys.* 347, 734–738.
- Ruden, S. P. and Pollack, J. B., 1991. The dynamical evolution of the protosolar nebula. *Astrophys. J.* 375, 740–760.
- Sekiya, M. 1998. Quasi-equilibrium density distributions of small dust aggregations in the solar nebula. *Icarus* 133, 298–309.
- Shakura, N. I. and Sunyaev, R. A., 1973. Black holes in binary systems. Observational appearance. *Astron. Astrophys.* 24, 337–355.
- Stepinski, T. F., 1998. The solar nebula as a process-an analytic model. *Icarus* 132, 100–112.
- Stepinski, T. F. and Valageas, P., 1996. Global evolution of solid matter in turbulent protoplanetary disks. I. Aerodynamics of solid particles. *Astron. Astrophys.* 309, 301–312.
- Stepinski, T. F. and Valageas, P., 1997. Global evolution of solid matter in turbulent protoplanetary disks. II. Development of icy planetesimals. *Astron. Astrophys.* 319, 1007–1019.
- Stevenson, D. J. and Lunine, J. I., 1988. Rapid formation of Jupiter by diffuse redistribution of water vapor in the solar nebula. *Icarus* 75, 146–155.
- Stone, J. M., Gammie, C. F., Balbus, S. A., and Hawley, J. F., 2000. Transport processes in protostellar disks. In Mannings, V., Boss, A. P., and Russell, S. S. (Eds.) *Protostars and Planets IV*, Univ. of Arizona Press, Tucson. pp. 589–612.
- Supulver, K. D. and Lin, D. N. C., 2000. Formation of icy planetesimals in a turbulent solar nebula. *Icarus* 146, 525–540.
- Takeuchi, T. and Lin, D. N. C. 2002. Radial flow of dust particles in accretion disks. *Astrophys. J.* 581, 1344–1355.
- Thommes, E. W., Duncan, M. J., and Levison, H. F., 1999. The formation of Uranus and Neptune in the Jupiter-Saturn region of the Solar System. *Nature* 402, 635–638.

- Weidenschilling, S. J., 1977a. Aerodynamics of solid bodies in the solar nebula. *Mon. Not. R. Astron. Soc.* 180, 57–70.
- Weidenschilling, S. J., 1977b. The distribution of mass in the planetary system and solar nebula. *Astrophys. Space Sci.*, 51, 153–158.
- Weidenschilling, S. J., 1980. Dust to planetesimals - Settling and coagulation in the solar nebula. *Icarus* 44, 172–189.
- Weidenschilling, S. J., 1984. Evolution of grains in a turbulent solar nebula. *Icarus* 60, 553–567.
- Weidenschilling, S. J., 1997. The Origin of comets in the solar nebula: A unified model. *Icarus* 127, 290–306.
- Weidenschilling, S. J., 2000. Formation of planetesimals and accretion of the terrestrial planets. *Space Sci. Rev.* 92, 295–310.
- Weidenschilling, S. J. 2003. Planetesimal formation in two dimensions: Putting an edge on the solar system. In *Lunar and Planetary Institute Conference Abstracts*, # 1707.
- Weidenschilling, S. J. and Cuzzi, J. N., 1993. Formation of planetesimals in the solar nebula. In Levy, E. H and Lunine, J. I., (Eds.) *Protostars and Planets III*, Univ. of Arizona Press, Tucson. pp.1031–1060.
- Youdin, A. N. and Chiang, E. I., 2004. Particle pileups and planetesimal formation. *Astrophys. J.* 601, 1109–1119.
- Yu, Y. and Hewins, R. H., 1998. Transient heating and chondrite formation - Evidence from sodium loss in flash heating simulation experiments. *Geochim. Cosmochim. Acta* 62, 159–172.
- Yurimoto, H. and Kuramoto, K., 2004. Molecular cloud origin for the oxygen isotope heterogeneity in the solar system. *Science* 305, 1763–1766.

Table 1: Definition of variables used in this paper.

Variable	Definition
a	Generic particle radius
a_1, a_2	Coefficients for evaporation rate
a_d, a_m, a_p	Radii of dust, migrators, and planetesimals
c_s	Sound speed
H	Nebular scale height
H_d, H_m	Half-thickness of the dust and migrator layers
m	Mass of a solid particle
m_d, m_m, m_p	Masses of individual dust, migrator, and planetesimal, bodies
\bar{m}	Average mass of a gas molecule
m_p	Mass of a proton
M_\odot	Mass of star
\dot{M}	Mass accretion rate onto the star
P_{eq}, P_{vap}	Equilibrium and actual pressure of water in the nebula
r	Distance from the star
S_{vap}, S_d, S_m, S_p	Source functions of vapor, dust, migrators and planetesimals
St	Stokes number
t	Time
T	Temperature of gas
T_e, T_m	Effective temperature and midplane temperature of the nebula
v_{drag}	Inward migration velocity of migrators due to gas drag
v_r	Advective velocity of the gas
v_{turb}	Turbulent velocity of the gas
Z	Evaporation rate of ice particles
γ	Ratio of gas specific heats
ν, ν_m	Viscosity/Diffusivity of the nebular gas and migrators
ρ_g	Mass density of gas at the nebular midplane
ρ_i	Mass density of ice
Σ, Σ_p	Surface density of the gas and planetesimals
τ	Optical depth from nebular midplane to surface
Ω	Keplerian angular rotation velocity

Table 2: Definition of parameters used in our model.

Parameter	Units	Definition
Σ_0	g/cm ²	Nebular gas surface density at 1 AU
p	-	Exponent of nebular surface density power law
R_0	AU	Initial radius of disk
α	-	Turbulence parameter
$t_{coag}(1 \text{ AU})$	years	Coagulation timescale to form migrators from dust at 1 AU
$t_{acc}(1 \text{ AU})$	years	Accretion timescale to form planetesimals from migrators at 1 AU
q^*	erg/g	Strength of solids

Table 3: Values of parameters used in the model runs presented here and mass remaining in disk and water at the end of the runs.

Parameter/Case	1	2	3	4	5	6	7
Σ_0	7×10^3	7×10^3	7×10^3	7×10^3	2.8×10^3	2.8×10^3	10^3
p	-1	-1	-1	-1	-1	-1	-0.5
R_0	40	40	40	40	100	100	56
α	10^{-4}	10^{-4}	10^{-4}	10^{-3}	10^{-4}	10^{-3}	10^{-3}
$t_{coag}(1 \text{ AU})$	10^4	10^5	10^5	10^4	10^5	10^5	10^4
$t_{acc}(1 \text{ AU})$	10^4	10^3	10^2	10^4	10^3	10^3	10^4
q^*	10^6	10^6	10^6	10^6	10^6	10^6	10^6
Disk Properties							
M_D start	$0.2M_\odot$	$0.2M_\odot$	$0.2M_\odot$	$0.2M_\odot$	$0.2M_\odot$	$0.2M_\odot$	$0.2M_\odot$
Length of model run	10^6 yrs	3×10^6 yrs	3×10^6 yrs	3×10^6 yrs	3×10^6 yrs	3×10^6 yrs	3×10^6 yrs
M_D end	$0.16M_\odot$	$0.14M_\odot$	$0.16M_\odot$	$0.06M_\odot$	$0.19M_\odot$	$0.10M_\odot$	$0.09M_\odot$
M_{H_2O} start	$302M_\oplus$	$302M_\oplus$	$302M_\oplus$	$302M_\oplus$	$302M_\oplus$	$302M_\oplus$	$302M_\oplus$
$M_{planetesimals}$ end	$5.8M_\oplus$	$47M_\oplus$	$156M_\oplus$	$4.9M_\oplus$	$62M_\oplus$	$27M_\oplus$	$8M_\oplus$
M_{solids} end	$41M_\oplus$	$126M_\oplus$	$233M_\oplus$	$6.9M_\oplus$	$244M_\oplus$	$142M_\oplus$	$16M_\oplus$

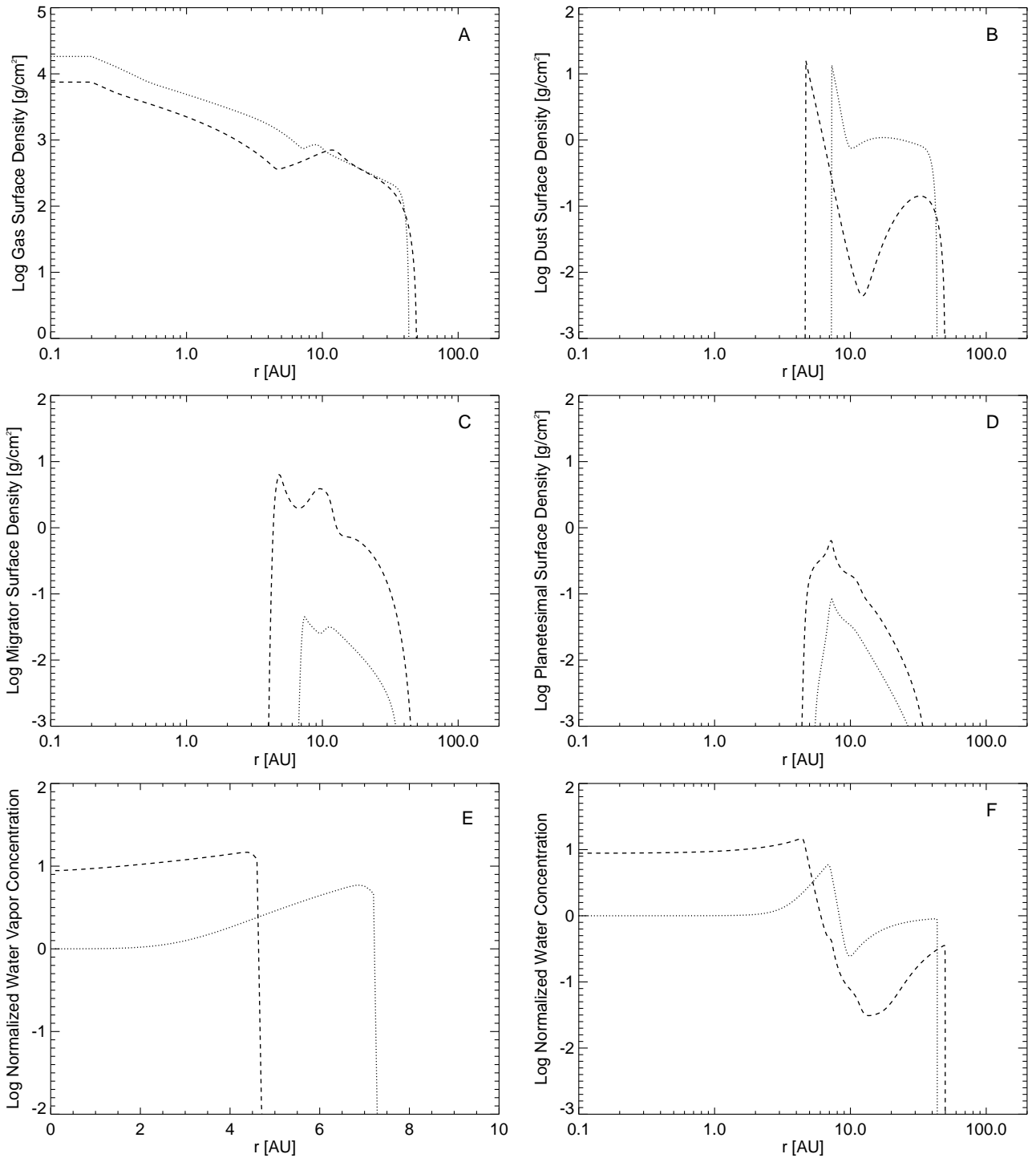


Figure 1: The evolution of the disk surface density (A), dust surface density (B), migrator surface density (C), planetesimal surface density (D), water vapor concentration (E), and total water concentration (F) for Case 1. Plotted are the distributions after 10^5 (dotted) and 10^6 (dashed) years.

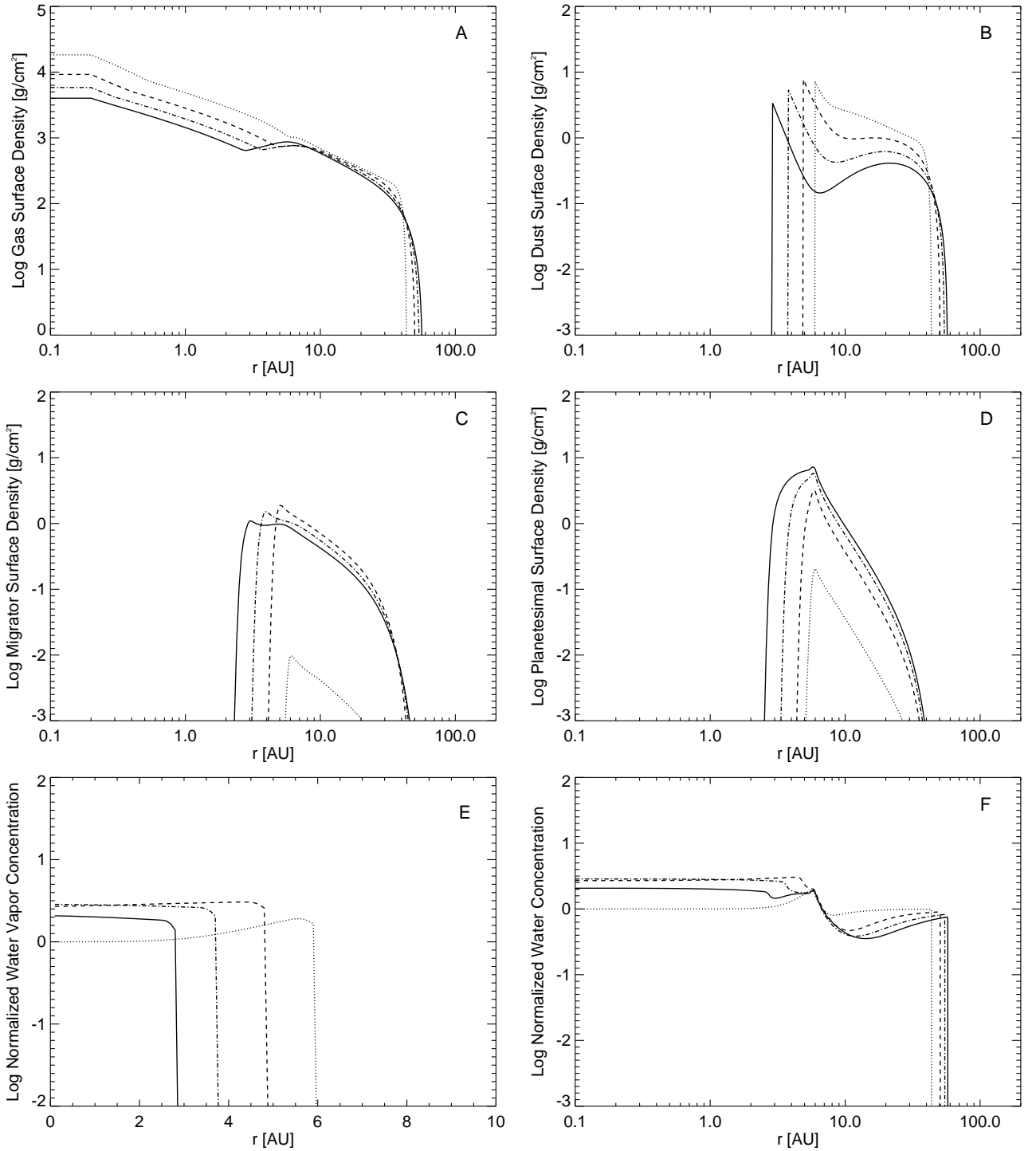


Figure 2: Disk and water evolution for Case 2. Same as Figure 1, with the 2×10^6 (dash-dot) and 3×10^6 (solid) years of evolution plotted.

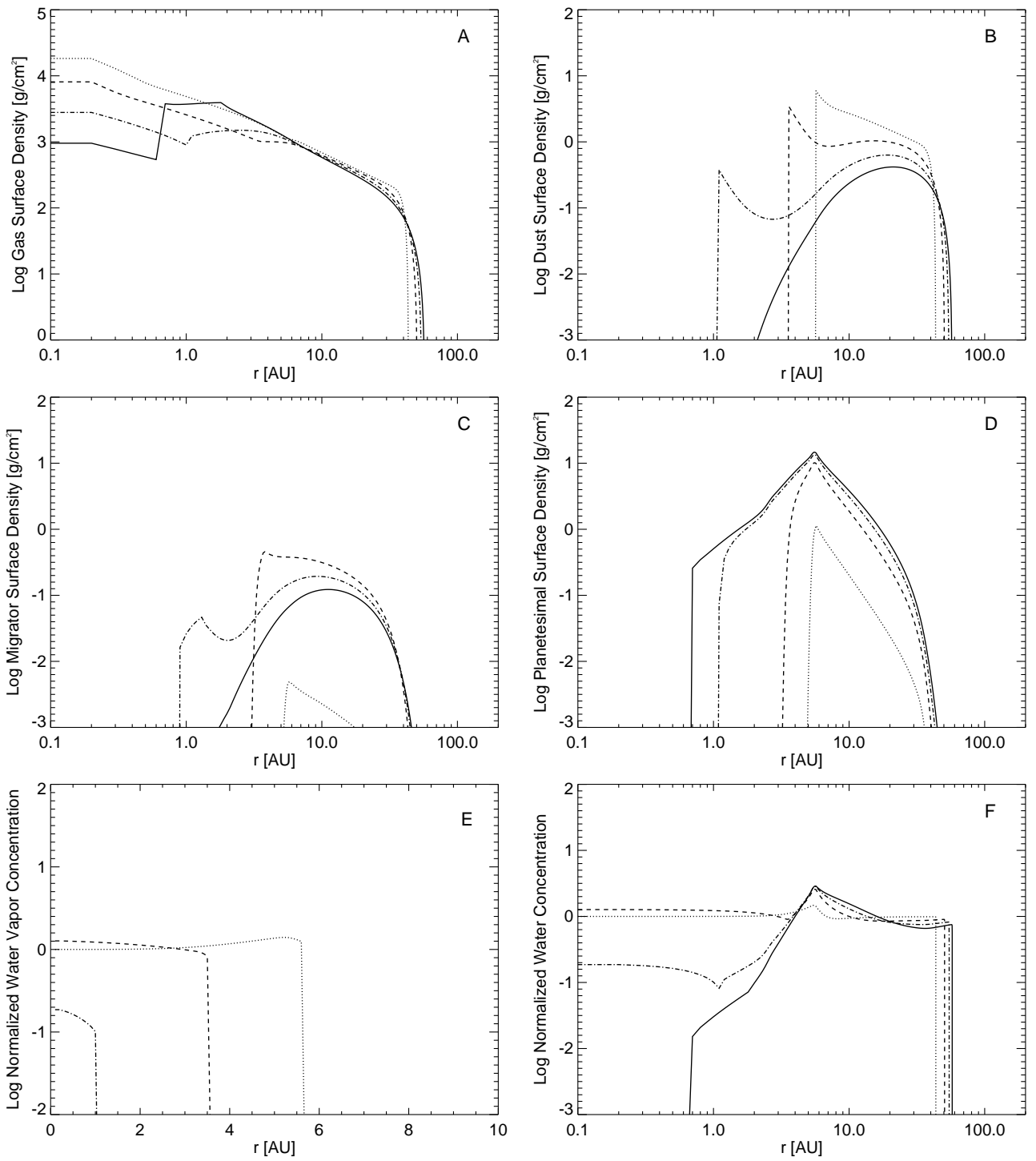


Figure 3: Disk and water evolution for Case 3. Same as Figure 2.

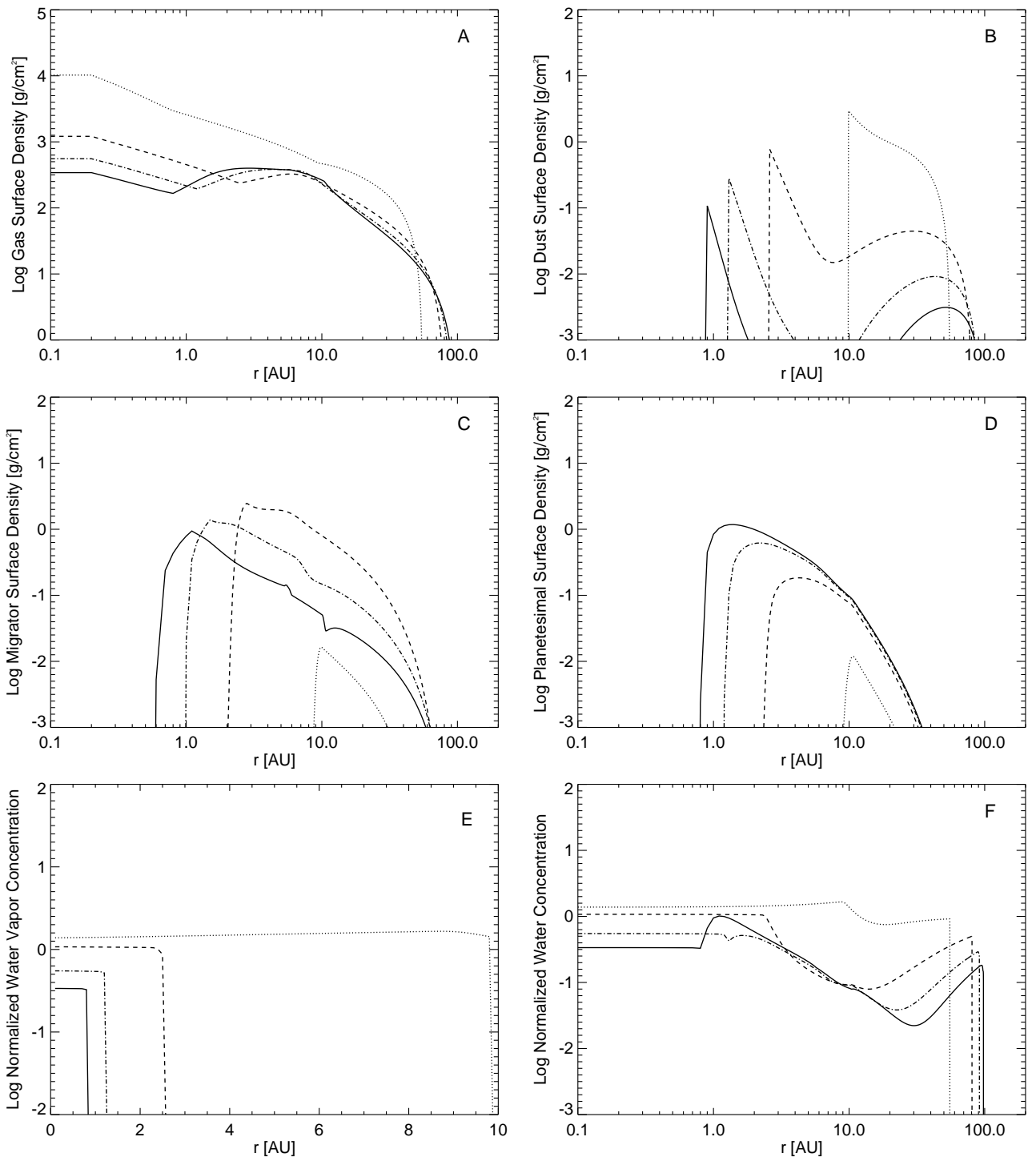


Figure 4: Disk and water evolution for Case 4. Same as Figure 2.

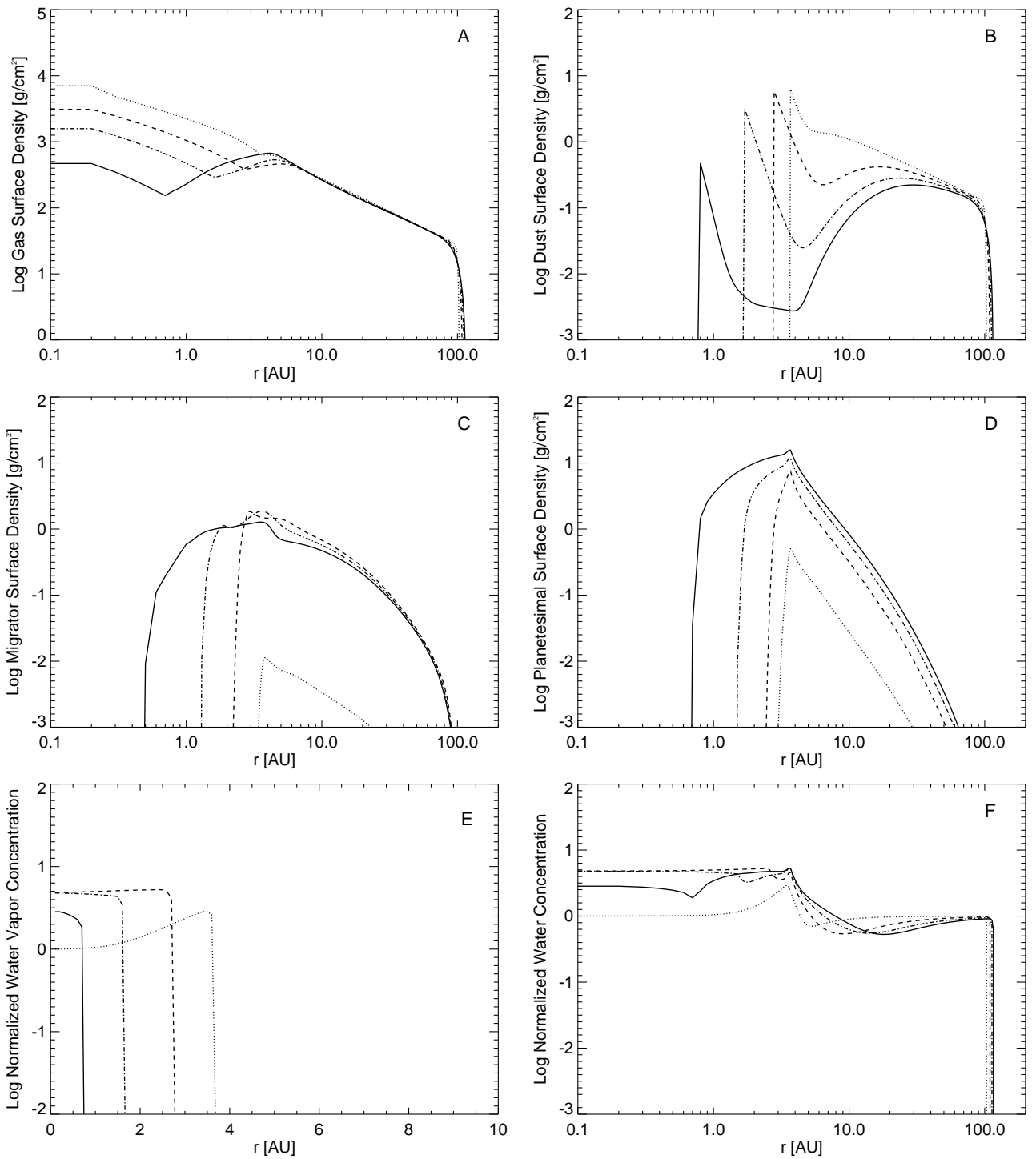


Figure 5: Disk and water evolution for Case 5. Same as Figure 2.

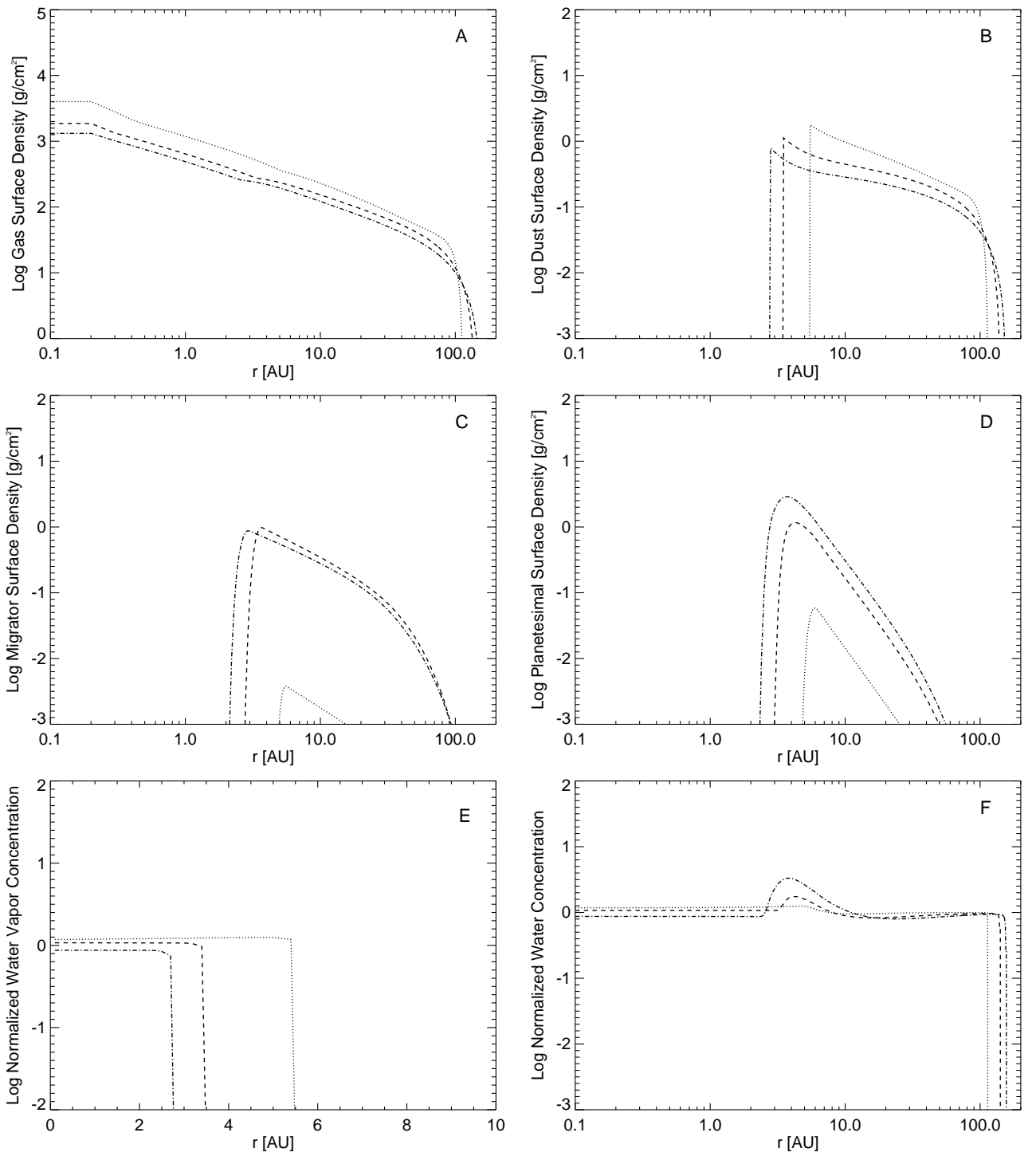


Figure 6: Disk and water evolution for Case 6. Same as Figure 2.

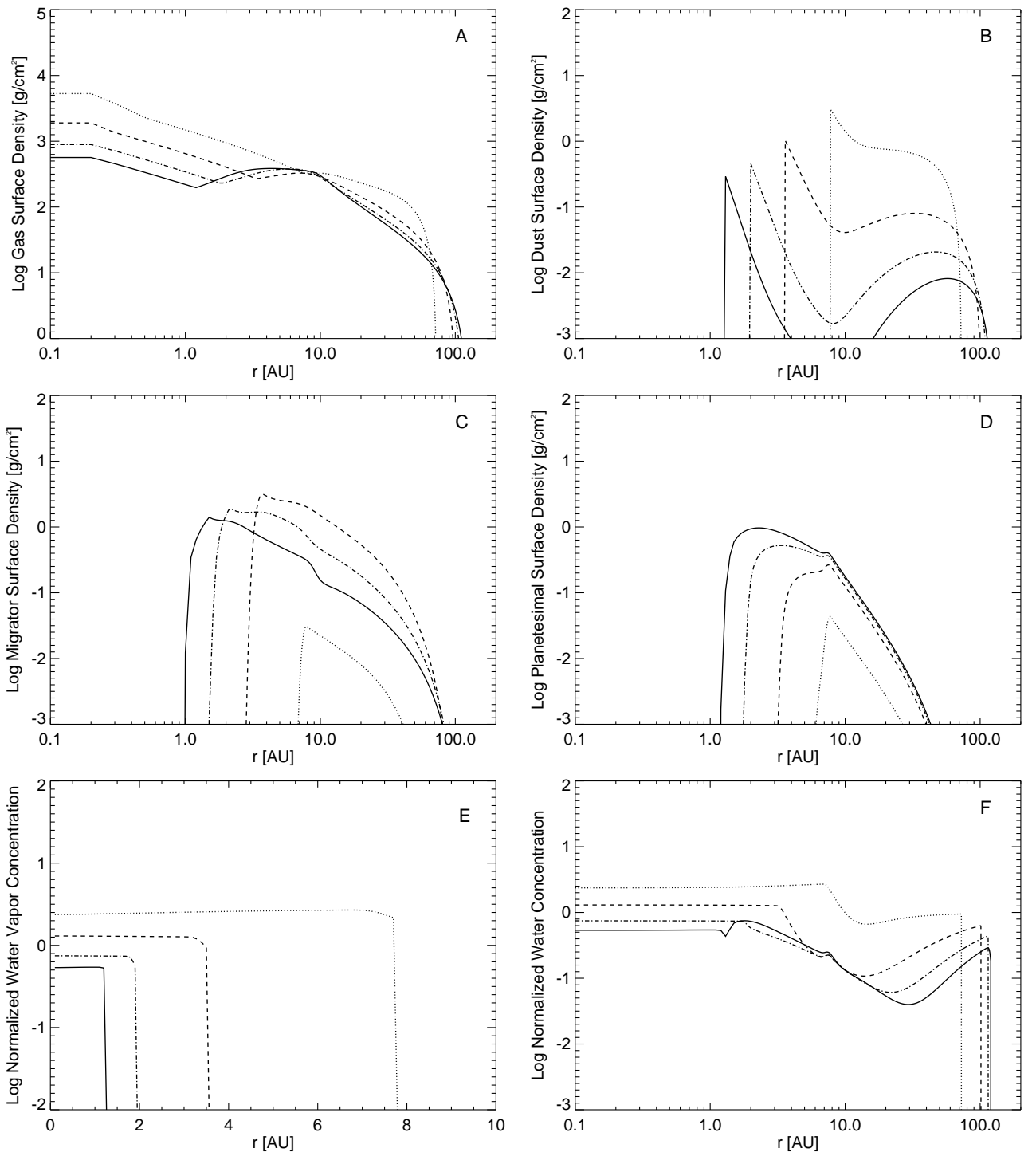


Figure 7: Disk and water evolution for Case 7. Same as Figure 2.